THE DYNAMIC RESPONSE OF FLUIDIC CIRCUITS WITH BLOCKED AND ORIFICE TERMINATED LINES

Bradley O. Montgomery

Air Force Institute of Technology
Wright-Patterson Air Force Base, Ohio

December 1971

UNITED STATES AIR FORCE

AIR UNIVERSITY

AIR FORCE INSTITUTE OF TECHNOLOGY

Wright-Patterson Air Force Base, Ohio

Unclassified

Security Classification

DOCUMENT CONTROL DATA - R & D

(Security classification of title, body of abstract and indexing annotation must be entered when the overall report is classified)

1. ORIGINATING ACTIVITY *(Corporate author)*

Air Force Institute of Technology (AFIT-SE)
Wright-Patterson AFB, Ohio 45433

2a. REPORT SECURITY CLASSIFICATION

Unclassified

2b. GROUP

3. REPORT TITLE

THE DYNAMIC RESPONSE OF FLUIDIC CIRCUITS WITH BLOCKED AND ORIFICE TERMINATED LINES

4. DESCRIPTIVE NOTES *(Type of report and inclusive dates)*

AFIT Thesis

5. AUTHOR(S) *(First name, middle initial, last name)*

Bradley O. Montgomery
1/Lt USAF

6. REPORT DATE	7a. TOTAL NO. OF PAGES	7b. NO. OF REFS
December 1971	58	20

8a. CONTRACT OR GRANT NO.	9a. ORIGINATOR'S REPORT NUMBER(S)
b. PROJECT NO.	GA/ME/72-2
c.	9b. OTHER REPORT NO(S) *(Any other numbers that may be assigned this report)*
d.	

10. DISTRIBUTION STATEMENT

Approved for public release; distribution unlimited.

11. SUPPLEMENTARY NOTES

Approved for public release; IAW AFR 190-17
JERRY C. HIX, Captain, USAF
Director of Information

12. SPONSORING MILITARY ACTIVITY

AFFDL/FGL

13. ABSTRACT

The dynamic response of a pneumatic circuit with mean flow was investigated experimentally in the 40-1050 Hz frequency range and the results compared with theory. All cases consisted of a 0.032 in ID line with either a blocked or orifice terminated end line. The orifice sizes used were 0.0135, 0.016 and 0.020 in ID with a length of 0.062 inches. The line was tested at pressures from 1.5 to 26.0 psig.

Comparison of experimental and theoretical results were made with a computer program using Nichols' equations as modified by Krishnaiyer and Lechner, with modification of attenuation for mean turbulent flow using Brown's work. A different orifice impedance model was used with mean turbulent flow than had been used with blocked or mean laminar flow. The experimental transfer gain was predicted within ± 1 db of theory for a blocked line, and within ± 2 db of theory for a mean laminar flow in the line. Experimental phase shift was predicted within ± 15° for a blocked line, and within 30° for mean laminar flow. With mean turbulent flow in the line, the gain was predicted within ± 2 db of theory for the two smallest orifices, and within ± 5 db of theory for the largest orifice, while the phase shift was predicted within ± 30° at frequencies less than 500 Hz, and within ± 70° at frequencies greater than 500 Hz.

Tb

DD FORM 1 NOV 65 1473

Unclassified

Security Classification

THE DYNAMIC RESPONSE OF FLUIDIC CIRCUITS WITH BLOCKED AND ORIFICE TERMINATED LINES

THESIS

Bradley O. Montgomery
GA/ME/72-2 1/Lt USAF

Ia.

THE DYNAMIC RESPONSE OF FLUIDIC CIRCUITS WITH BLOCKED AND ORIFICE TERMINATED LINES

THESIS

Presented to the Faculty of the School of Engineering

of the Air Force Institute of Technology

Air University

In Partial Fulfillment of the

Requirements for the Degree of

Master of Science

by

Bradley O. Montgomery, B.S.A.E.

1/Lt USAF

Graduate Astronautical Engineering

December 1971

Approved for public release; distribution unlimited

I C

Preface

This thesis is the ninth that has been written at AFIT in a continuing study of the frequency response characteristics of pneumatic transmission lines. The primary purpose of this report was to obtain experimental results for a series fluidic circuit with and without mean air flow. The experimental results were then compared with existing theory for verification.

To achieve this evaluation, the computer program which was used by Malanowski (Ref 12) was modified for increased attenuation with turbulent flow based on one of the several studies by Brown (Ref 3).

I would like to thank the many people who made this report possible. In particular, I would especially like to thank Dr. M. E. Franke, my thesis and faculty advisor, who extended my knowledge of fluidics and provided suggestions and help when they were needed.

I would also like to thank my wife, Barbara, for patience and understanding as well as her proof-reading and typing.

Bradley O. Montgomery

Contents

List of Figures

List of Tables

List of Symbols

Symbol	Description	Units
A	line cross-sectional area	in^2
Beta	Phase angle	degrees
C	capacitance/unit length	$\frac{cis\text{-}sec}{psi}/in$
C_{al}	adiabatic capacitance/unit length; $A/\lambda P$	$\frac{cis\text{-}sec}{psi}/in$
C_{el}	Nichols capacitance parameter	$\frac{cis\text{-}sec}{psi}/in$
d	inside diameter of line	in
db	line gain	decibels
g	dynamic pressure ratio, P_r/P_s	dimensionless
G	conductance/unit length	$\frac{cis}{psi}/in$
G_{el}	isothermal conductance/unit length; $8\pi\nu_T/\lambda P$	$\frac{cis}{psi}/in$
h_ν	velocity distribution parameter	dimensionless
h_T	temperature distribution parameter	dimensionless
ID	line inside diameter	in
j	$\sqrt{-1}$	dimensionless
L	inductance/unit length	$\frac{psi/sec}{cis}/in$
L_{sl}	cross section inertance/unit length; ρ/A; $L_{el} = 1/3\ L_{sl}$	$lbf\text{-}sec^2/in^5$
ℓ	length of line	in
N_r	Reynolds number based on diameter	dimensionless
$\overline{P}$	DC (Mean) pressure)	psi

Symbol	Description	Units
P	AC pressure	psi-rms
Q	volumetric flow rate	cis
R	resistance/unit length	$\frac{\text{psi}}{\text{cis}}/\text{in}$
R_v	viscous resistance/unit length; $\omega_\nu L_{sl} = 8\pi\mu/A^2$; $R_{el} = R_{vl}$	$\frac{\text{psi}}{\text{cis}}/\text{in}$
T	temperature	°R
$\dot{V}_{p_\sigma}$	phase velocity without wall effects	in/sec
x	distance from load	in
Y	shunt admittance/unit length	$\frac{\text{cis}}{\text{psi}}/\text{in}$
Z	impedance/unit length	$\frac{\text{psi}}{\text{cis}}/\text{in}$
Z_c	characteristic impedance	$\frac{\text{psi}}{\text{cis}}/\text{in}$
α	attenuation/unit length	neper/in
β	phase shift/unit length	rad/in
Γ	propagation constant/unit length	1/in
γ	ratio of specific heats	dimensionless
λ	wavelength	in
μ	dynamic viscosity	psi-sec
ν	kinematic viscosity	in^2/sec
ν_T	thermal diffusivity	in^2/sec
ρ	density	$\text{lb}_f\text{-sec}^2/\text{in}^4$
σ^2	Prandtl number	dimensionless
Ω	frequency; $R^2\omega/\nu$	dimensionless
ω	angular frequency	rad/sec
ω_ν	viscous characteristic frequency; $8\pi\nu/A$	rad/sec
ω_T	thermal characteristic frequency; $\omega_\nu/\sigma^2 = 8\pi\nu_T/A$	rad/sec

Subscripts

$( )_{amb}$	ambient
$( )_{c}$	characteristic
$( )_{end}$	end value of the line
$( )_{fm}$	flow meter
$( )_{L}$	load properties
$( )_{m}$	main line properties
$( )_{o}$	orifice properties
$( )_{r}$	receiving end properties
$( )_{s}$	sending end properties
$( )_{t}$	transducer properties
$( )_{1,2,...10}$	1, 2, ..., 10th line property with reference to line diagram schematic

Abstract

The dynamic response of a pneumatic circuit with mean flow was investigated experimentally in the 40-1050 Hz frequency range and the results compared with theory. All cases consisted of a 0.032 in ID line with either a blocked or orifice terminated end line. The orifice sizes used were 0.0135, 0.016 and 0.020 in ID with a length of 0.062 inches. The line was tested at pressures from 1.5 to 26.0 psig.

Comparison of experimental and theoretical results were made with a computer program using Nichols' equations as modified by Krishnaiyer and Lechner, with modification of attenuation for mean turbulent flow using Brown's work. A different orifice impedance model was used with mean turbulent flow than had been used with blocked or mean laminar flow. The experimental transfer gain was predicted within ± 1 db of theory for a blocked line, and within ± 2 db of theory for a mean laminar flow in the line. Experimental phase shift was predicted within ± 15° for a blocked line, and within ± 30° for mean laminar flow. With mean turbulent flow in the line, the gain was predicted within ± 2 db of theory for the two smallest orifices, and within ± 5 db of theory for the largest orifice, while the phase shift was predicted within ± 30° at frequencies less than 500 Hz, and within ± 70° at frequencies greater than 500 Hz.

THE DYNAMIC RESPONSE OF FLUIDIC CIRCUITS WITH BLOCKED AND ORIFICE TERMINATED LINES

I. Introduction

Background

Fluidic systems and control devices are becoming increasingly important in many engineering applications. Because of their adaptability to extreme environmental conditions, their simplicity of operation and light weight, they are ideally suited for many applications where these features are desirable or needed. But, before an engineer is able to use fluidic systems and control devices he must first be able to accurately predict the dynamic characteristics of pneumatic transmission lines.

Many good mathematical models have been developed to predict the dynamic characteristics of pneumatic transmission lines. Iberall's model, (Ref 8), was probably the most important and it led to simplified solutions in the developments of Berg and Tijdeman, Brown, Nichols, and Rohmann and Grogan (Refs 1, 2, 16, and 18).

Nichols' equations gave an accurate prediction of the frequency response of pneumatic transmission lines, and several studies (Refs 7, 9, 13, and 20) have shown good experimental agreement for blocked lines. Krishnaiyer and Lechner (Ref 11) modified Nichols' equations to obtain better accuracy at low frequencies, and found good correlation between experimental and theoretical results with mean air flow. Malanowski (Ref 12) found good experimental agreement with theory for branched

pneumatic transmission lines with blocked and orifice terminated lines. Brown (Ref 3) developed a mean turbulent flow model which predicts increased attenuation over that predicted by mean laminar flow.

Problem

The dynamic characteristic of series connected pneumatic transmission lines have been studied extensively in the laminar region of mean flow, but since turbulent flow will also be encountered in some applications, more study is needed in this area. The equations used for mean laminar flow will not give good results for mean turbulent flow at all frequencies, unless increased attenuation is used.

Objectives

The objectives of this study were as follows:

1. The development of a computer program based on the theoretical equations which would:

   a. allow for series and parallel connected lines,

   b. use the modification of Nichols' equations as presented by Malanowski in his thesis (ref 12), with increased attenuation for mean turbulent flow from Brown's work (Ref 3).

2. An experimental investigation to determine how useful the above theoretical model is with mean air flow and with a blocked line using the following conditions:

   a. frequency variation from 40 to 1050 Hz,

   b. small cross sectional area line (.032 inch ID) with varying orifice size and blocked.

II. Theory

From electrical transmission line theory, the relationship between voltage and current at any point in the line is given by (Ref 19)

$$\frac{dV}{dx} = ZI \tag{1}$$

and

$$\frac{dI}{dx} = YV \tag{2}$$

If the voltage is replaced by pressure and current by volumetric flow rate, we have an analogy for a pneumatic transmission line, and equations (1) and (2) become

$$\frac{dP}{dx} = ZQ = (R + j\omega L)Q \tag{3}$$

and

$$\frac{dQ}{dx} = YP = (G + j\omega C)P \tag{4}$$

where $R = Re(Z)$, $G = Re(Y)$, $L = \frac{1}{\omega} Im(Z)$ and $C = \frac{1}{\omega} Im(Y)$.

The solutions to (3) and (4) are

$$P(x) = B_1 e^{-\Gamma x} + B_2 e^{\Gamma x} \tag{5}$$

and

$$Q(x) = \frac{B_1}{Z_c} e^{-\Gamma x} - \frac{B_2}{Z_c} e^{\Gamma x} \tag{6}$$

where $\Gamma = \alpha + j\beta = Re(\Gamma) + jIm(\Gamma)$ and B_1 and B_2 are constants determined by the boundary conditions on the line.

The model of Nichols (Ref 16) defined two characteristic frequencies and two distribution parameters which included the effects of frequency dependent losses in the pneumatic lines, assuming rigid line walls and no mean flow. These were

$$\omega_\nu = \frac{8\pi\nu}{A} \tag{7}$$

$$\omega_T = \frac{8\pi\nu_T}{A} = \frac{\omega_\nu}{\sigma^2} \tag{8}$$

$$h_\nu = 2\sqrt{\omega/\omega_\nu} \tag{9}$$

and

$$h_T = 2\sqrt{\omega/\omega_T} \tag{10}$$

Nichols' development resulted in the following equations

$$Z = j\omega L_{sl} + R_{vl}\left[\frac{R_{el}}{R_{vl}} + j\frac{\omega L_{el}}{R_{vl}}\right] \tag{11}$$

and

$$Y = j\omega C_{al} + \frac{j\omega(\gamma-1)\,C_{al}}{\frac{(\gamma-1)\,C_{al}}{C_{el}} + \frac{j\omega(\gamma-1)\,C_{al}}{G_{el}}} \tag{12}$$

where

$$\frac{R_{el}}{R_{vl}} + j\frac{\omega L_{el}}{R_{vl}} = j\frac{h_\nu^2}{4}\left[\frac{1}{1-J(h_\nu\sqrt{2})} - 1\right] \tag{13}$$

and

$$\frac{(\gamma-1)\,C_{al}}{C_{el}} + j\frac{(\gamma-1)\,C_{al}}{G_{el}} = \frac{1}{J(h_T\sqrt{2})} = \frac{1}{J(\sigma h_\nu)} \tag{14}$$

Krishnaiyer and Lechner (Ref 11) developed approximations to the Bessel functions in equations (13) and (14), which would give greater accuracy at low frequencies. They are

$$\frac{R_{el}}{R_{vl}} = \frac{3}{8} + \frac{1}{4} h_\nu + \frac{3}{8} \cdot \frac{1}{h_\nu} \equiv DR \tag{15}$$

$$\frac{\omega L_{el}}{R_{vl}} = \frac{1}{4} h_\nu - \frac{15}{64} \cdot \frac{1}{h_\nu} \equiv DL \tag{16}$$

$$\frac{(\gamma-1)\, C_{al}}{C_{el}} = \frac{1}{4} + \frac{1}{2} h_T + \frac{1}{4} \cdot \frac{1}{h_T} \equiv DC \tag{17}$$

$$\frac{\omega(\gamma-1)\, C_{al}}{G_{el}} = \frac{1}{2} h_T - \frac{1}{4} \cdot \frac{1}{h_T} \equiv DG \tag{18}$$

With these definitions, equations (11) and (12) may be written as

$$Z = \frac{8\pi\mu}{A^2} [DR] + j \left[\frac{\omega\rho}{A} \div \frac{8\pi\mu}{A^2} [DL] \right] \tag{19}$$

and

$$Y = \frac{\omega(\gamma-1) \frac{A}{\gamma P} [DG]}{[DC]^2 + [DG]^2} + j\omega \left[\frac{A}{\gamma P} + \frac{(\gamma-1) \frac{A}{\gamma P} [DC]}{[DC]^2 + [DG]^2} \right] \tag{20}$$

For practical applications the approximations given in equations (15), (16), (17), and (18), give good results for $0.1\ \omega_\nu < \omega < \infty$.

An orifice ended fluid transmission line which has a mean air flow must be modeled differently than either a blocked line ($Z_{end} = \infty$) or an open line ($Z_{end} = 0$). Krishnaiyer and Lechner showed that good results could be obtained if the orifice ended line was modeled as

$$Z_{end} = \frac{\overline{P}_{end}}{Q_{end}} + j0 = Z_o \qquad (21)$$

If the mean flow in the line becomes turbulent, Brown (Ref 3) showed that the attenuation in the line will increase. This increase of α as a function of increasing Reynolds Number and frequency is shown in Figure 1, where Vp_o is the phase velocity without wall effects. As can be seen from Figure 1, as line diameter decreases, the effects of turbulent flow become more important at any given Reynolds Number. Figure 1 is part of Figure 2 from Brown's study (Ref 3), and is for the high frequency model. For low-frequency disturbances the flow is quasi-steady, but for high-frequency disturbances the turbulence level profile across the tube presumably does not rise and fall significantly, because of the inertia of the turbulent motion which forces a lag in the response to changes in the mean velocity profile. The break frequency, according to Brown, between high and low frequency occurs at about ($\Omega > 0.017(N_r)^{0.84}$). If Ω is less than this value, then the constant I-R-C model, shown in Figure 2 of Brown's study (Ref 3), should be used. Other restrictions on Figure 1, require the traveling waves to have wavelengths $\lambda >> 2\pi R$ (roughly $\lambda > 20R$) to prevent coupling between the wavelengths of the sine wave and the turbulence. Also, to prevent the turbulent fluctuations from being influenced by the propagating sine waves requires that $\Omega < 0.5N_r$. Brown states that the analysis should be adequate, though not so accurate, for frequencies up to ten times higher than this value.

If the velocity of the flow in the line becomes too great, then the resonant frequency of the line will change. This change of resonant

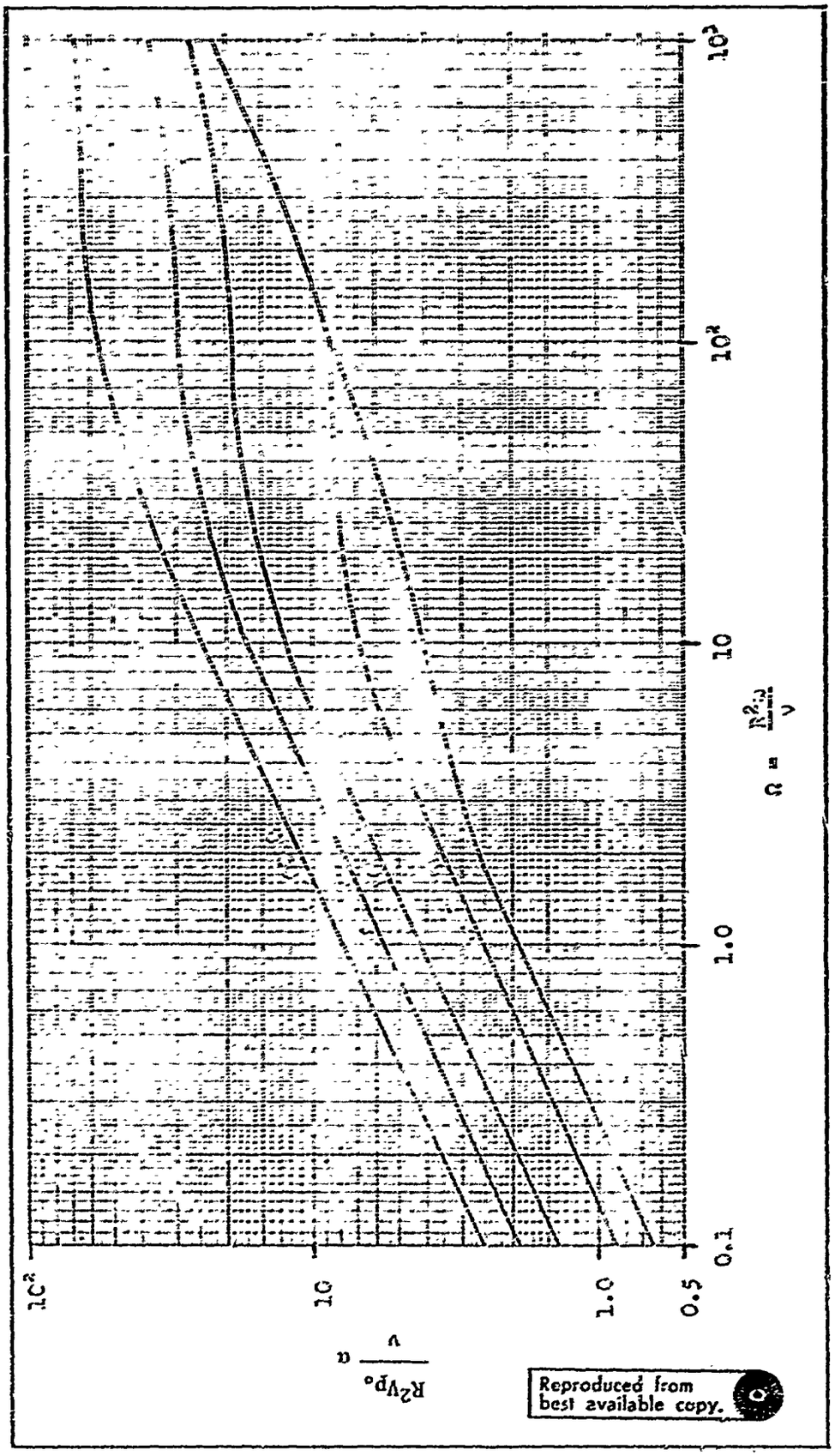

Fig 1 Predictions of attenuation factor for invariant turbulent flow without effects of heat transfer

frequency is equal to the sending frequency times $(1-M^2)$, where M is the Mach number of the flow in the line (Ref 15).

Krishnaiyer and Lechner found using Nichols' development and assuming ideal gas, small fluctuations and no flow that the transfer pressure gain for a pneumatic line is

$$\frac{P_r}{P_s} = \frac{2 Z_c Z_r e^{-\Gamma \ell}}{Z_c(Z_r + Z_c) + Z_c(Z_r - Z_c)e^{-\Gamma \ell}} \tag{22}$$

where

$$Z_c = \sqrt{Z/Y} \tag{23}$$

and

$$\Gamma = \sqrt{ZY} \tag{24}$$

They also showed that the input or sending impedance of the line is given by

$$Z_s = Z_c \frac{(Z_r + Z_c) + (Z_r - Z_c) e^{-\Gamma \ell}}{(Z_r + Z_c) - (Z_r - Z_c) e^{-\Gamma \ell}} \tag{25}$$

Equations (19), (20), (22), and (25) are sufficient to obtain reasonably accurate predictions of the complex properties of fluidic lines.

The gain between any two points in a cascaded line system can be shown to be the multiple of the gains for each line in the system. This is

$$g = \prod_{i=1}^{n-1} \left| \frac{P_{i+1}}{P_i} \right| \tag{26}$$

or given in decibels

$$g_{db} = 20 \log_{10} g \tag{27}$$

The phase angle for a cascaded line fluid system with reflected waves is

$$\text{Beta} = -\sum_{i=1}^{n-1} \tan^{-1} \left[\frac{\text{imaginary part of } \frac{P_{i+1}}{P_i}}{\text{real part of } \frac{P_{i+1}}{P_i}} \right] \tag{28}$$

The computer program used by Malanowski (Ref 12), was modified for increased attenuation with turbulent flow using the graph in Figure 1 from Brown's study (Ref 3).

III. Experimental Apparatus

The test system used was essentially the same as that used by Malanowski (Ref 12). The apparatus consisted of a pneumatic signal source, the monitoring equipment, and the test line configurations. Shown in Fig 2 is a schematic diagram of the overall setup, and Fig 3 shows a general view of the actual laboratory setup.

Pneumatic Signal Source

The major components of the pneumatic signal source consisted of an electronic signal generator, a power amplifier, and an electro-pneumatic signal generator.

A sinusoidal voltage was developed in the electronic signal generator in one of the wave analyzers. This voltage was amplified by a linear amplifier, and fed to a matched gain push-pull amplifier in the pneumatic signal generator for further amplification. The amplified signal was then used to operate a piezoelectric flapper valve in the pneumatic driver head, shown in Fig 4. The flapper valve creates a sinusoidal pressure pulse which varies about the mean pressure of through air flow in the pneumatic driver head.

Monitoring Equipment

The sinusoidal signal input frequency was monitored on an electronic counter, and the RMS amplitude of this signal was measured with a VTVM. The output of the static pressure transducer ($\bar{P}_L$) was monitored on a differential voltmeter, which allowed a constant observation of the mean line pressure.

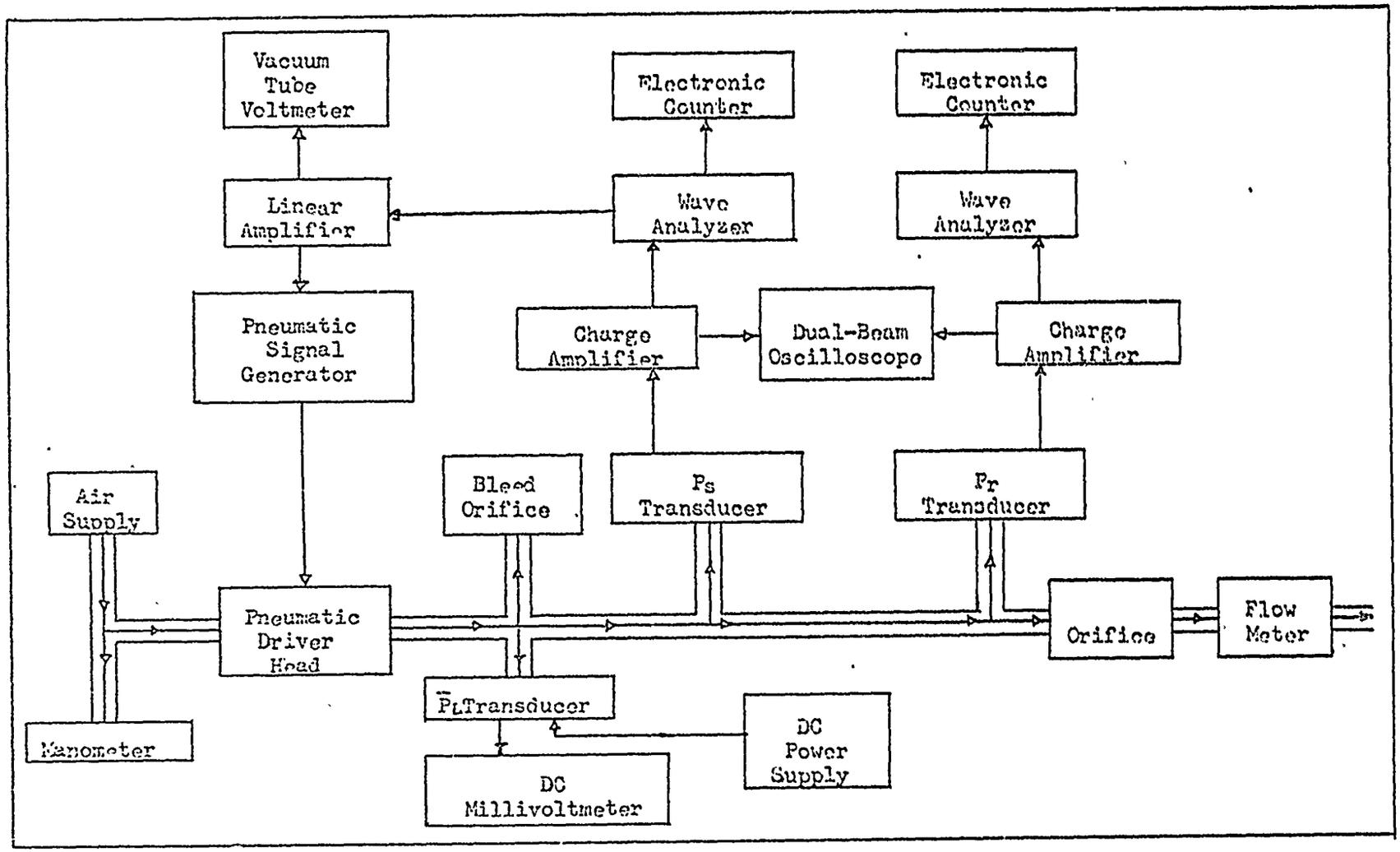

Fig 2 Schematic Diagram of Experimental Apparatus

Fig 3 General View of Apparatus

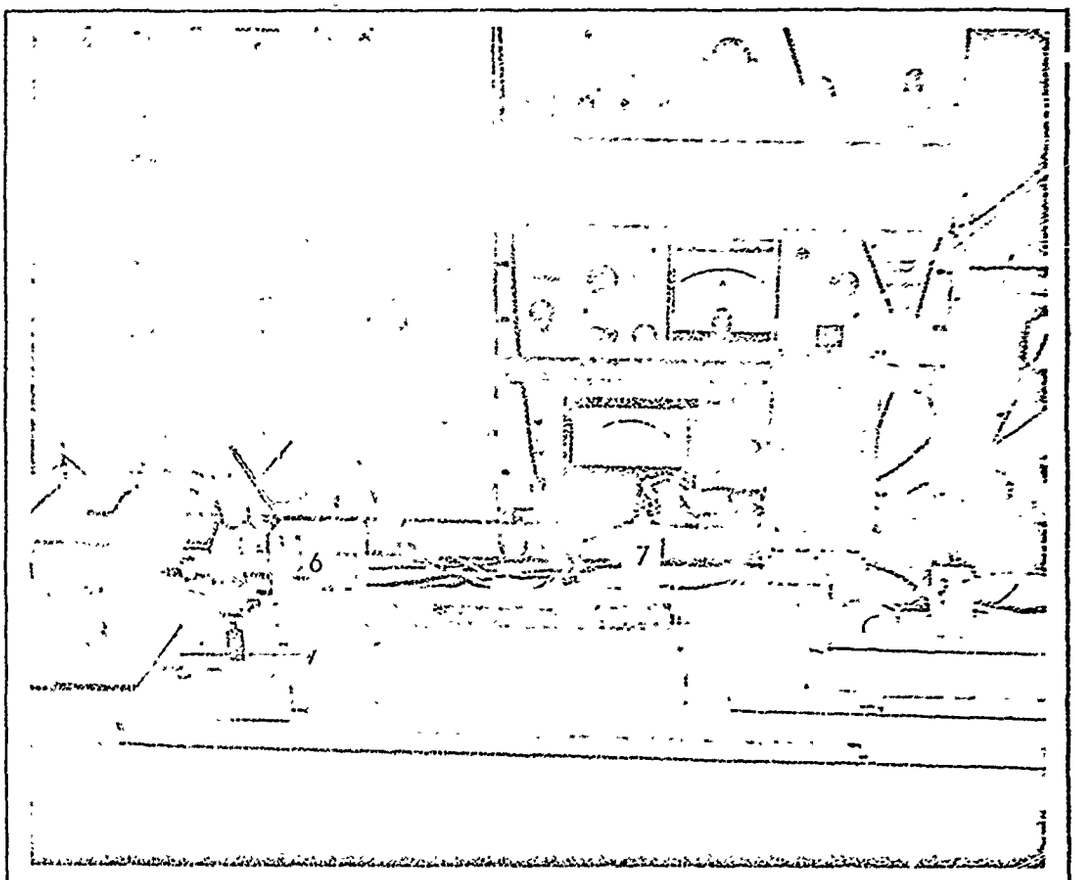

1. Pneumatic Driver Head
2. Dynamic Pressure Transducer (P_s)
3. Dynamic Pressure Transducer (P_r)
4. Mean Pressure Transducer ($\bar{P}_L$)
5. Bleed Orifice
6. Sending Fixture
7. Receiving Fixture

Fig 4 Pneumatic Driver and Sending Fixture

Two mercury-in-glass manometers were used to measure mean line pressure at the dynamic pressure ports ($\overline{P}_s$ and $\overline{P}_r$) before each experimental test. A rotometer type flow meter was used to measure volumetric flow rate at the terminating orifice of the line.

The quartz type sending and receiving dynamic pressure transducers fed their output to charge amplifiers. These amplified signals were then fed to wave analyzers for RMS voltage measurements. Both wave analyzers sent an output to an associated electronic counter to insure that both wave analyzers were operating at the same frequency.

A detailed description of the monitoring equipment is given by Wilda (Ref 20).

Test Configurations

The test line used for the experiment was stainless steel tubing of 0.032 in. ID, terminated with either a blocked end or an orifice. The orifice sizes used were 0.0135, 0.016, and 0.020 in. ID. The test line was made of solid one-piece construction as far as possible, with the only connection being where the orifice was soldered on to the main line. This one-piece construction was used to increase accuracy in the measurements of all line sections, which is critical if accurate test results are to be obtained. Figure 4 shows the test line connected to the pneumatic driver head. Detailed descriptions for each of the line setups are given in Appendix B.

IV. Experimental Procedures

To insure stability of the electrical signals, a warm-up period of approximately two hours was allowed for the equipment before making any test runs. Essentially the same test procedure was used for all tests.

The data recorded for each test run were Tamb, Pamb, $\overline{P}_s$, $\overline{P}_r$, P_s, P_r, P_L, Q_{fm}, and frequency. Mercury-in-glass manometers were connected to each dynamic pressure port to measure the mean pressure ($\overline{P}_s$ and $\overline{P}_r$). For those tests involving mean flow, the flow rate was measured and plotted against $\overline{P}_r$. These plots for the three different orifice sizes are shown in Figure 5, along with a plot for the 0.0135 orifice with an assumed orifice coefficient of 0.6. From the difference between the $\overline{P}_s$ and $\overline{P}_r$ values, the pressure drop was accounted for by dividing the line into a finite number of short sections each with a constant pressure. The pressure was assumed to drop linearly with distance from the P_s port to the P_r port, and with the same linear value from the P_r port to the orifice. The P_r transducer volume was input into the computer program as a small line in parallel with the main line.

The frequency of the input signal was varied from 40-1050 Hz, and values of P_s and P_r were measured on the wave analyzers, along with phase angle measurements from the dual beam oscilloscope. With each frequency change, the wave analyzer receiving the P_r signal was also changed to the new frequency, by observing the electronic counter and adjusting the wave analyzer until the value of both (P_r and P_s) electronic counters read the same. This was done to insure that the receiving wave analyzer was locked-on to the proper frequency.

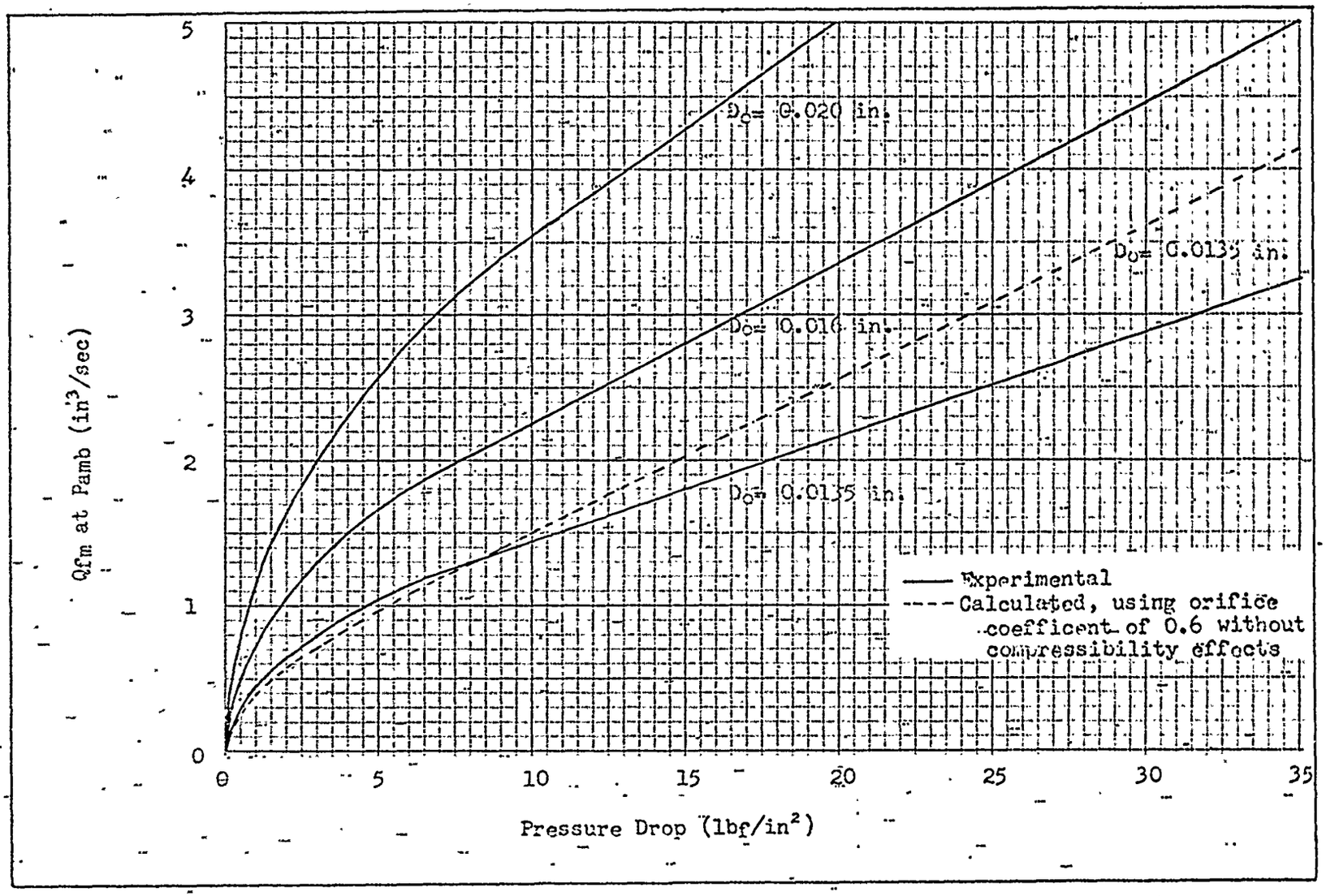

Fig 5 Q_{fm} versus $\bar{P}_r$ for different orifices.

By observing the sending and receiving signals on the dual-beam oscilloscope, the phase angle measurements were obtained by determining the linear distance the receiving signal had shifted with respect to the sending signal.

The recorded values of frequency, P_s, P_r, and phase angle were input to the computer program for comparison with theory. A Calcomp plotter graphed experimental and theoretical gain and phase angle versus frequency.

Signal Size

The signal size in this study was arbitrarily defined to be

$$S = \frac{P_s \text{ @f = 1000 Hz in psi-rms}}{\text{PL in psig}} \times 100$$

in percent. On the basis of this definition the signal size varied from 0.2 to 1.0 percent for this study.

V. Results and Discussion

Tables I and II give experimental data and test configuration data for all the experimental cases considered in this report. Appendix A contains theoretical frequency response curves for all cases not considered in this section, and Appendix B contains complete line dimension data for each case. Values of ω_v for this study ranged from approximately 280 to 700 rad/sec.

Table I

Experimental Data

Case Number	$\bar{P}_s$ psig	$\bar{P}_r$ psig	$\bar{P}_{end}$ psig	Q_{end} cis	Q_{fm} cis	Reynolds Number	Signal Size %
1	7.00	7.00	7.00	0.00	0.00	0000	0.5
2	15.00	15.00	15.00	0.00	0.00	0000	0.4
3	4.79	4.00	3.92	0.74	0.94	1494	0.5
4	9.04	8.01	7.91	0.84	1.31	2091	0.3
5	14.91	12.97	12.75	0.87	1.65	2634	0.2
6	21.02	18.76	18.51	0.91	2.09	3337	0.2
7	27.80	25.15	24.87	0.93	2.56	4077	0.2
8	2.85	1.83	1.71	0.90	1.01	1605	0.7
9	7.64	5.45	5.20	1.23	1.68	2669	0.3
10	14.42	10.85	10.50	1.36	2.36	3750	0.2
11	1.63	0.64	0.53	0.89	0.92	1467	1.0
12	5.13	2.36	2.03	1.51	1.72	2743	0.5
13	9.33	4.63	4.18	1.87	2.42	3859	0.3

Table II
Test Configurations

Case Number	Orifice Diameter in.	Complete Line Dimensions	Results
1	0.0000	Table III	Figs 6 and 7
2	0.0000	Table III	Figs 18 and 19
3	0.0135	Table IV	Figs 10 and 11
4	0.0135	Table IV	Figs 8 and 9
5	0.0135	Table IV	Fig 15
6	0.0135	Table IV	Figs 20 and 21
7	0.0135	Table IV	Figs 16 and 17
8	0.0160	Table V	Figs 22 and 23
9	0.0160	Table V	Fig 24
10	0.0160	Table V	Figs 25 and 26
11	0.0200	Table VI	Figs 27 and 28
12	0.0200	Table VI	Fig 29
13	0.0200	Table VI	Figs 30 and 31

Blocked Line

Blocked line tests were run first on the fluidic circuit to insure proper modeling of the circuit, and to insure the computer program was working properly. Blocked line tests were known to give good agreement between theory and experiment (refs 7 and 12). Typical results for the blocked line tests are shown in Figures 6 and 7, and additional results are shown in Appendix A. Experimental agreement with theory for the blocked line tests was within ±1 db for the gain, and within ±15 degrees for the phase shift, for those cases where the signal size was less than 0.5 percent. For signal sizes greater than 0.5 percent, the difference

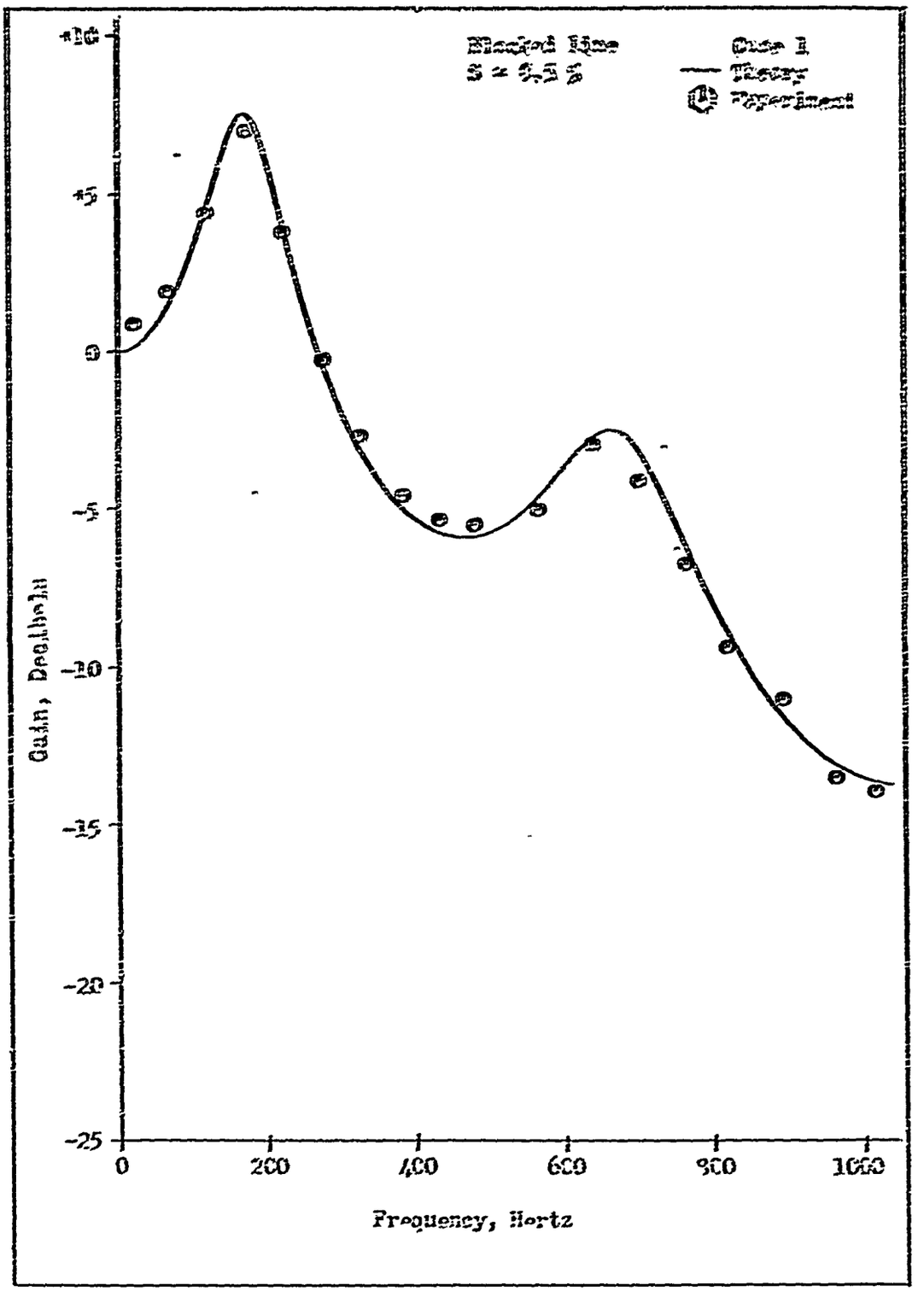

Fig 6 Correlation of Experimental Results with Theory for Blocked Line

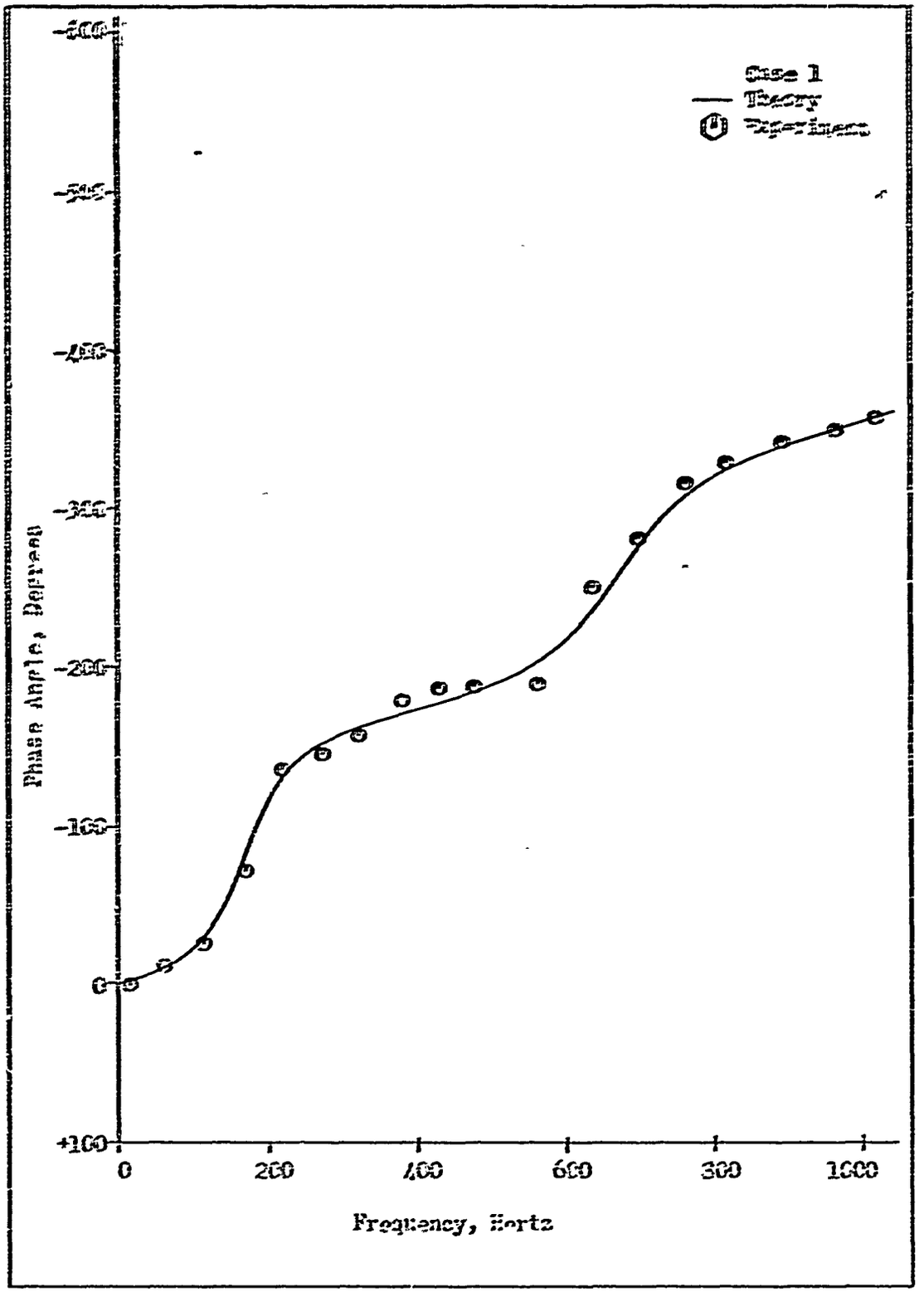

Fig 7 Correlation of Experimental Results with Theory for Blocked Line

between theory and experiment tended to increase as the signal size increased. The approximate experimental error in measuring the phase shift and gain was ±15° and ±1 db. This is the same as the variation of these values for the blocked flow tests.

Laminar Flow

Typical dynamic pressure gain and phase angle measurements for a mean laminar flow are shown for the 0.0135 in ID orifice in Figures 8 and 9. Results in the mean laminar flow region for this orifice at small signal size were within ±1 db for the gain and ±30° for the phase shift. Gain and phase angle measurements for the larger orifices had to be taken at signal sizes larger than 0.7 percent, to obtain signals large enough to read from the wave analyzers. As the signal size increased above 0.5 percent, the difference between theoretical and experimental values increased. Shown in Figures 10 and 11 are the results for an experimental run for the 0.0135 in ID orifice with a signal size of 0.5 percent. Other results for large signal sizes are shown in Appendix A. Table II gives the signal sizes for all experimental cases.

Transition Region Flow

The transition region of mean flow, as determined by the Reynolds number, occurred at different values of Reynolds number for the three different orifices sizes. The transition region of mean flow was also evident, by a randomly fluctuating P_T signal on the oscilloscope. The value of the Reynolds number for the transition region decreased with increasing orifice size. For the 0.0135 in ID orifice the transition

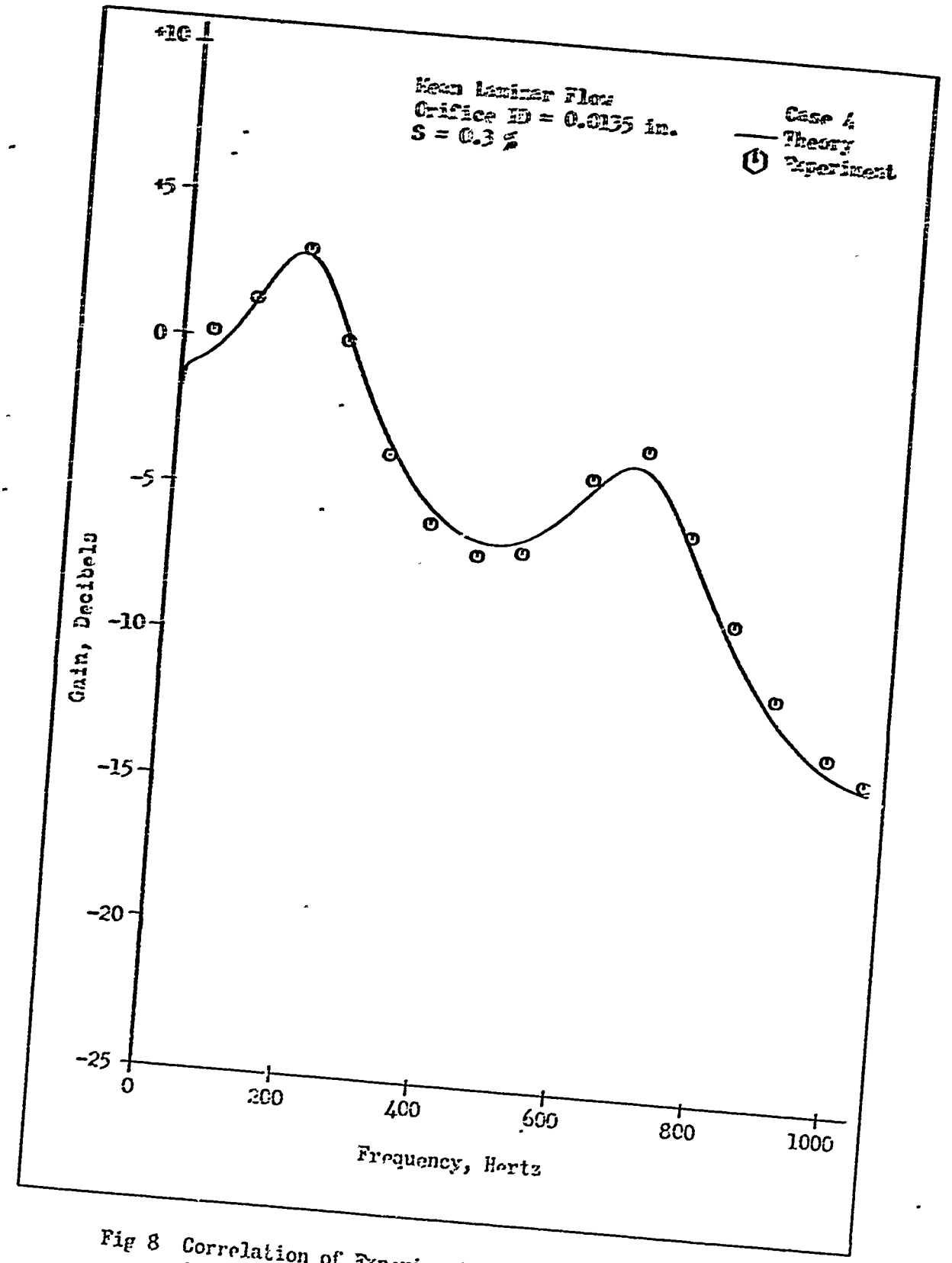

Fig 8 Correlation of Experimental Results with Theory for 0.0135 in ID orifice

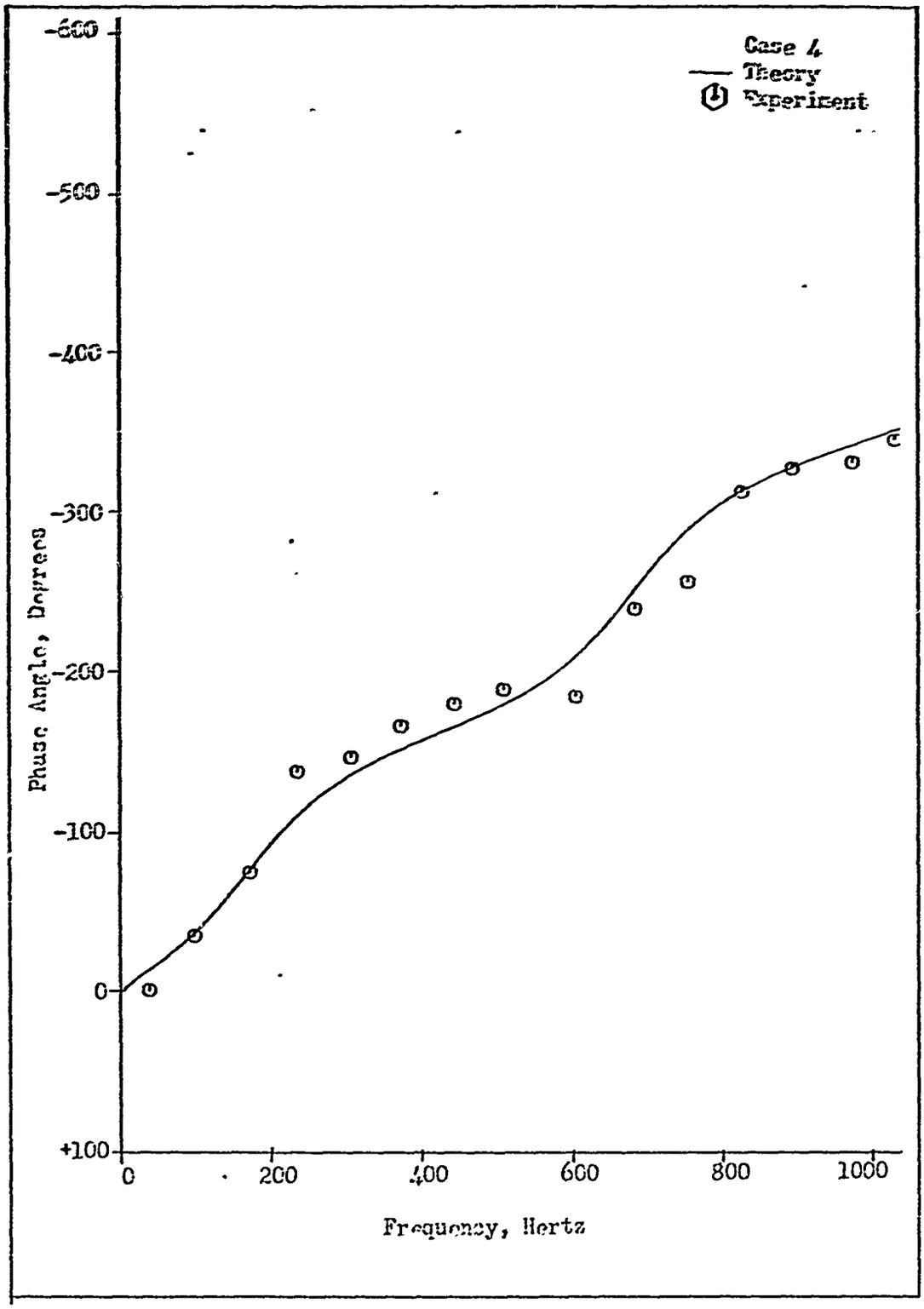

Fig 9 Correlation of Experimental Results with Theory for 0.0135 in ID orifice

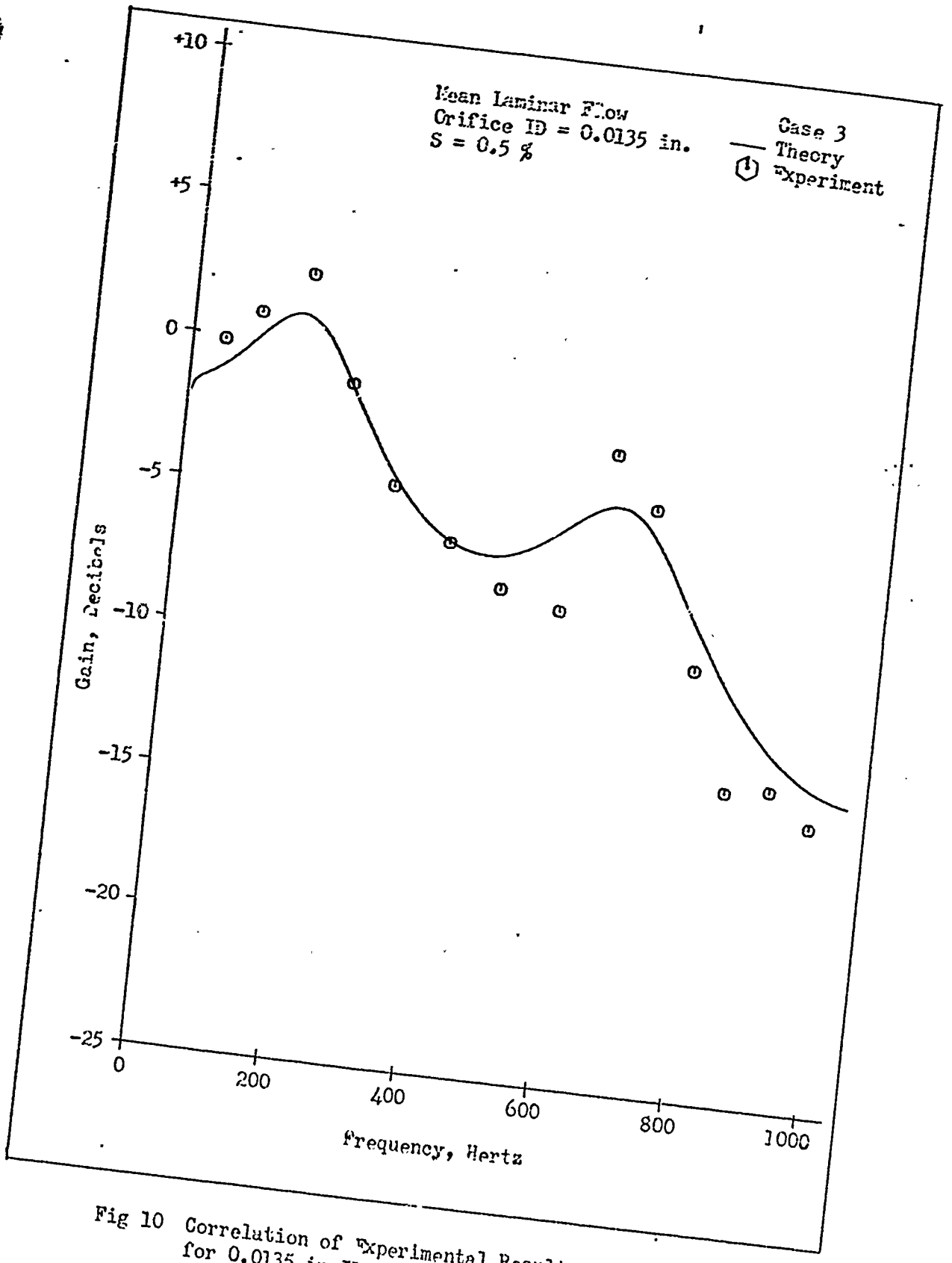

Fig 10 Correlation of Experimental Results with Theory for 0.0135 in ID orifice

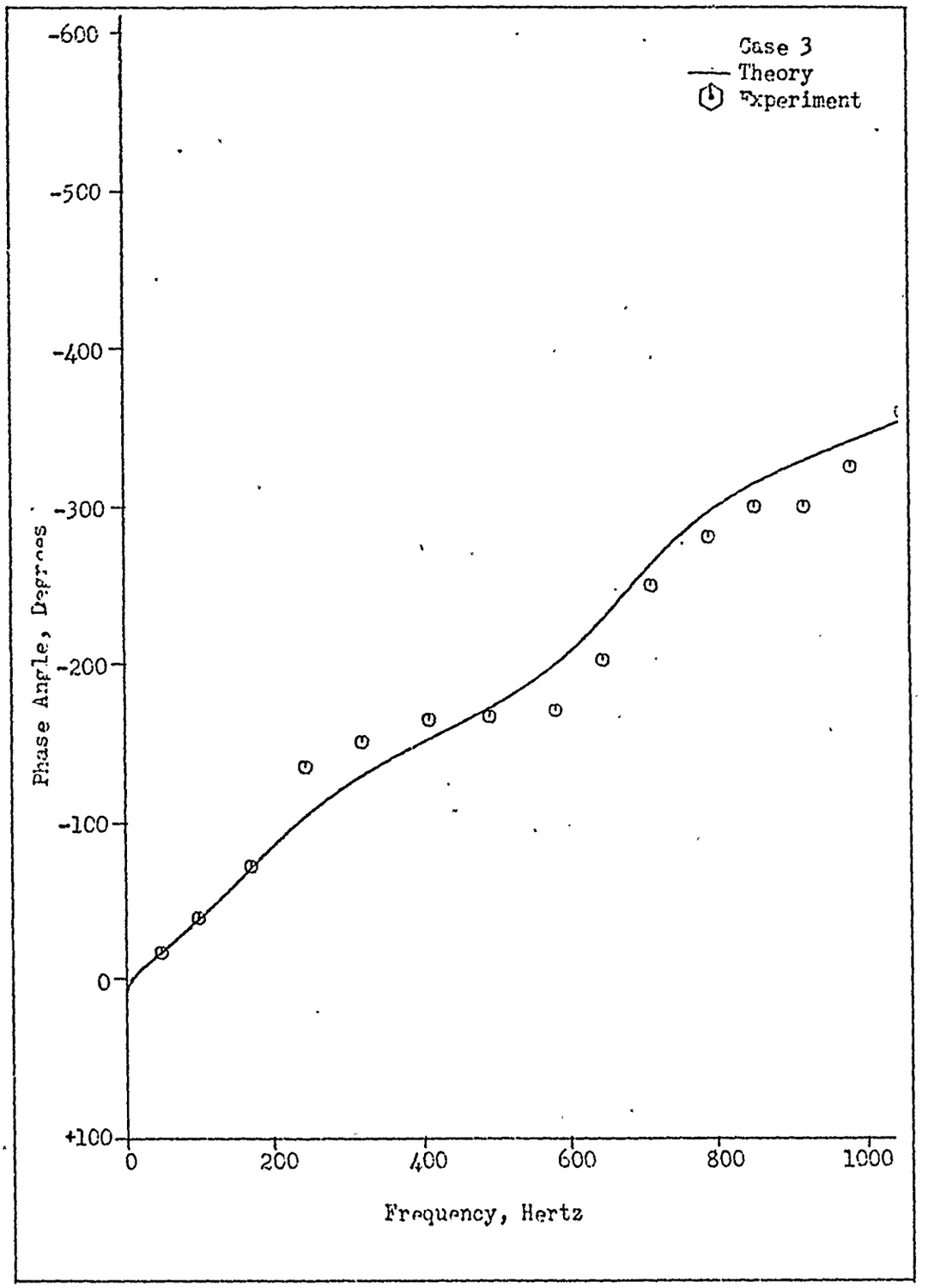

Fig 11 Correlation of Experimental Results with Theory for 0.0135 in ID orifice

region occurred in the Reynolds number range of approximately 2100-3000. For the 0.016 in ID orifice, transition occurred in the range of approximately 1700-2900, and for the 0.020 in ID orifice, 1500-2800.

The P_r readings on the wave analyzer in the transition region fluctuated as much as 30 percent of the meter scale at times. The fluctuation was particularly bad at frequencies below 250 Hz, but tended to lessen as the frequency was increased above 300 Hz. When fluctuating signals were present, the P_r readings were taken by averaging the high and low values of the fluctuation. The P_r readings on the oscilloscope were impossible to read in the transition region of mean flow, because of the fluctuating signal. A typical example of a randomly fluctuating P_r signal during mean transition flow is shown in Figure 12.

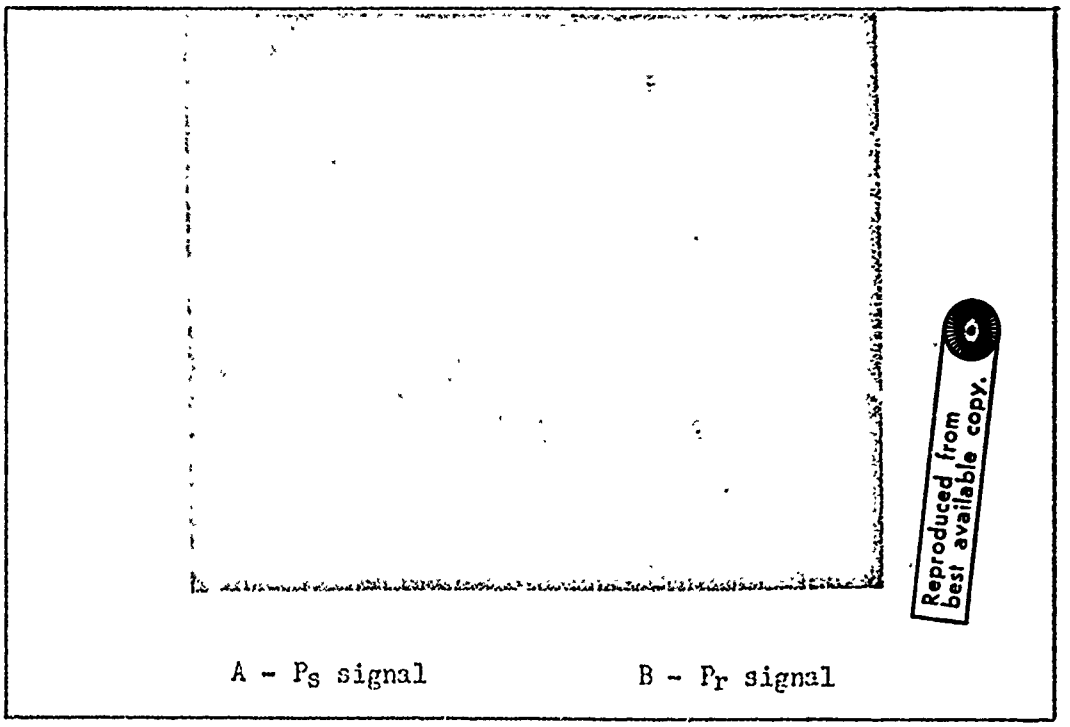

Fig 12 Typical Oscilloscope Trace for Mean Transition Flow at a frequency of 350 Hz

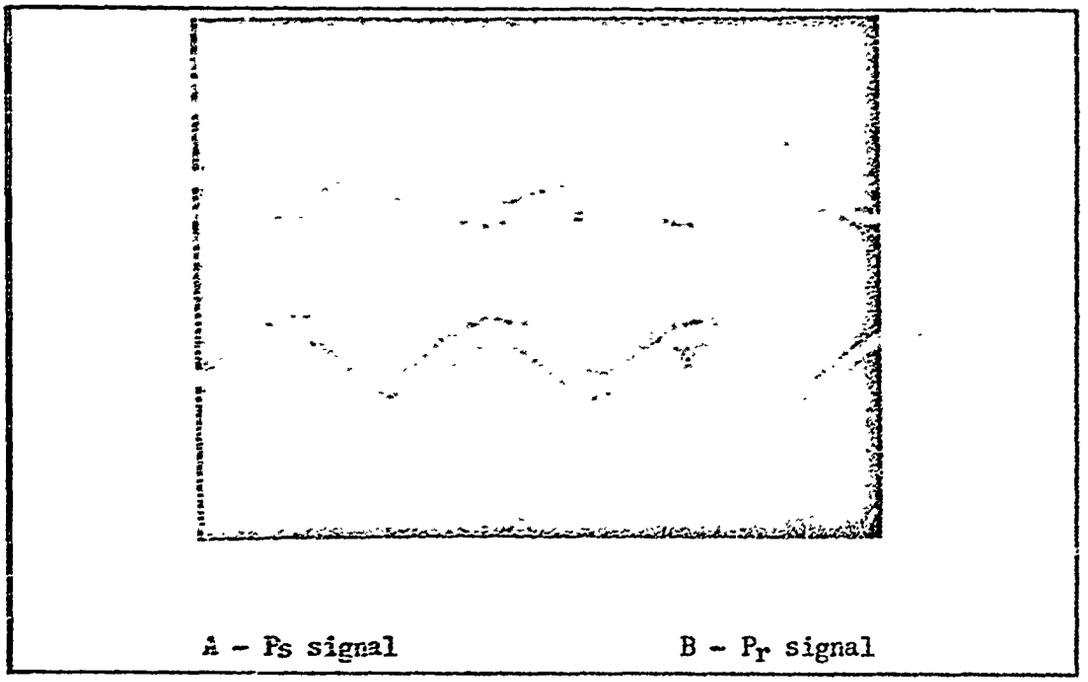

Fig 13 Typical Oscilloscope Trace for Mean Laminar Flow at a Frequency of 350 Hz

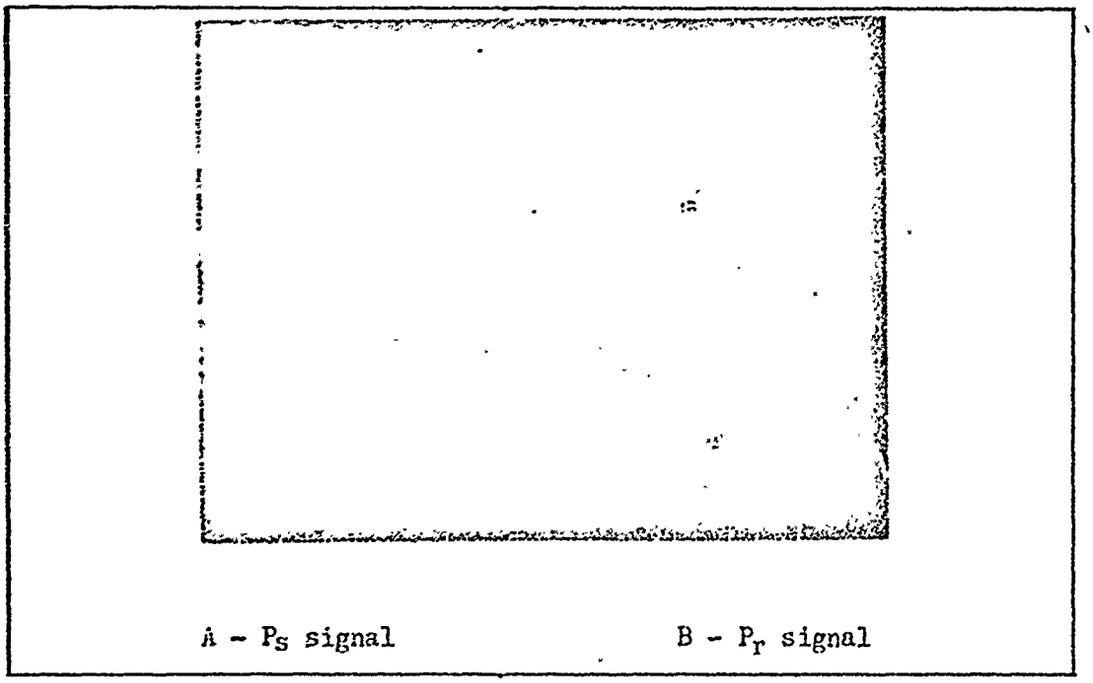

Fig 14 Typical Oscilloscope Trace for Mean Turbulent Flow at a Frequency of 350 Hz

Typical P_r and P_s signals with mean laminar flow and mean turbulent flow present are shown in Figures 13 and 14 respectively. Because of the randomly fluctuating P_r signal, no phase angle measurements were attempted in mean transition flow. Also, no calculations for increased attenuation was attempted for mean transition flow cases. Experimental results for the 0.0135 in ID orifice in mean transition flow along with the theoretical values are shown in Figure 15. Additional results for the 0.016 and 0.020 in ID orifices are shown in Appendix A. Results varied for the three different sized orifices, with the two smallest sized orifices agreeing within ±2 db, except at low frequency (40-200 Hz) for the 0.0135 in ID orifice where the theory was 2-4 db higher than the experimental values. Experimental results for the 0.020 in ID orifice varied ±5 db from theory.

Turbulent Flow

Typical dynamic pressure gain and phase angle measurements for a mean turbulent flow are shown in Figures 16 and 17 for the 0.0135 in ID orifice. The theoretical curve labeled with an L was calculated using the same theory that was used to obtain the blocked, laminar and transition theoretical curves in this report. As can be seen from Figure 16, the experimental results do not agree with this theory except at frequencies above 700 Hz, where agreement is fairly good. Values of the ratio of turbulent attenuation to laminar attenuation were obtained from Figure 1, and plotted for Reynolds numbers from 2500-4000 in increments of 500. These plots were then input into the computer program as second order polynomial equations, and the attenuation calculated by the computer program using the theoretical equations was increased for the

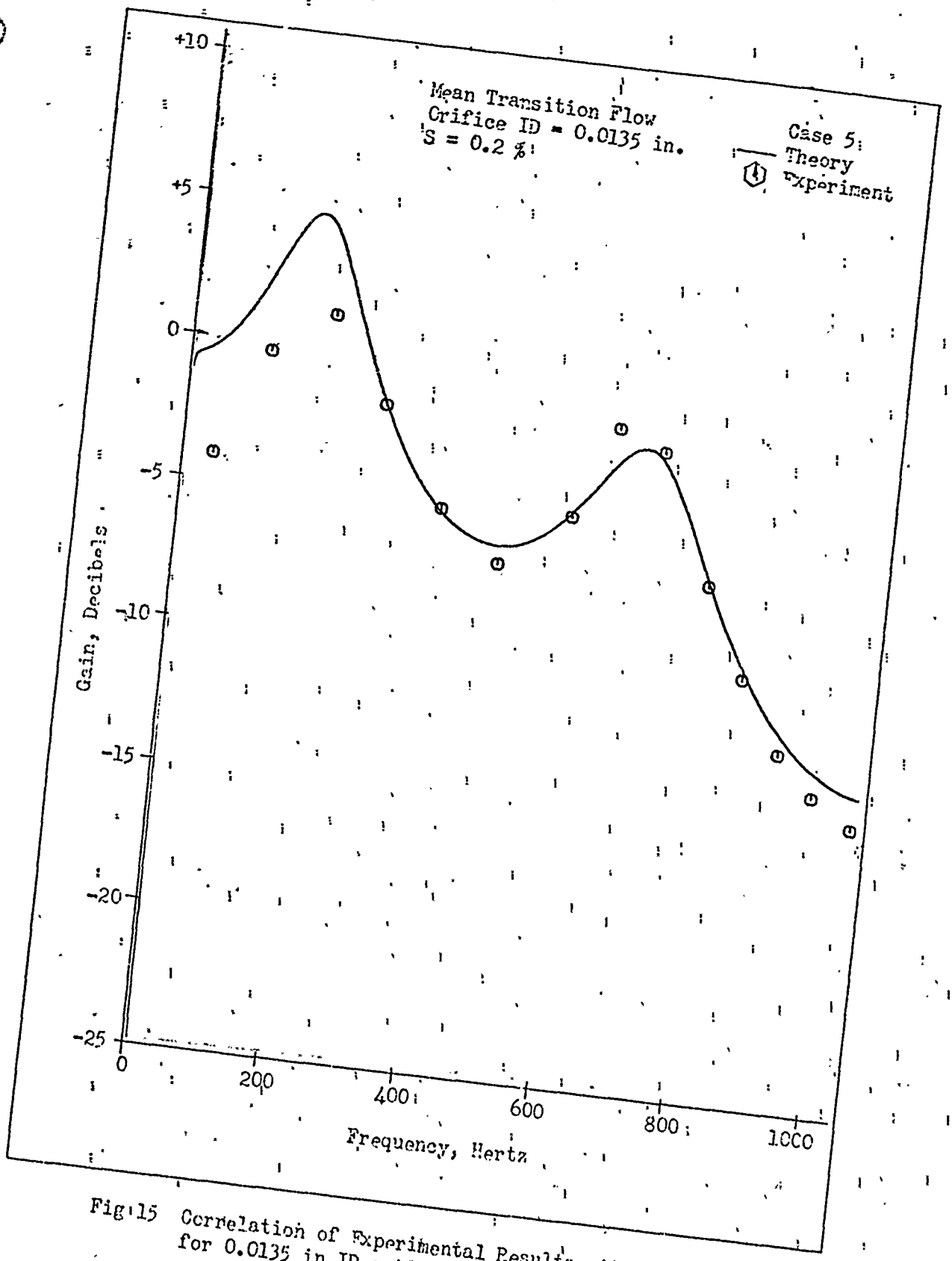

Fig 15 Correlation of Experimental Results with Theory for 0.0135 in ID orifice

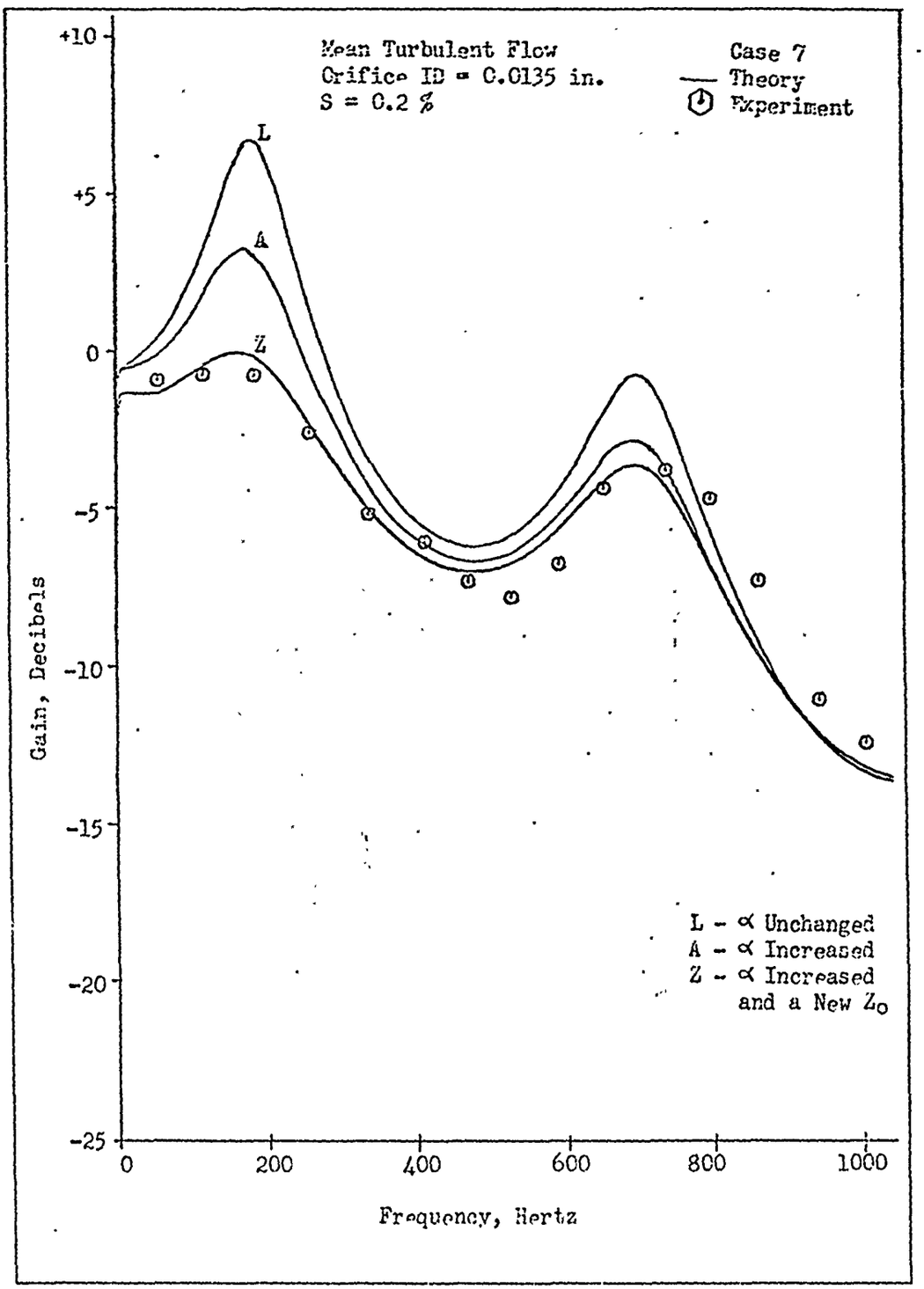

Fig 16 Correlation of Experimental Results with Theory for 0.0135 in ID orifice

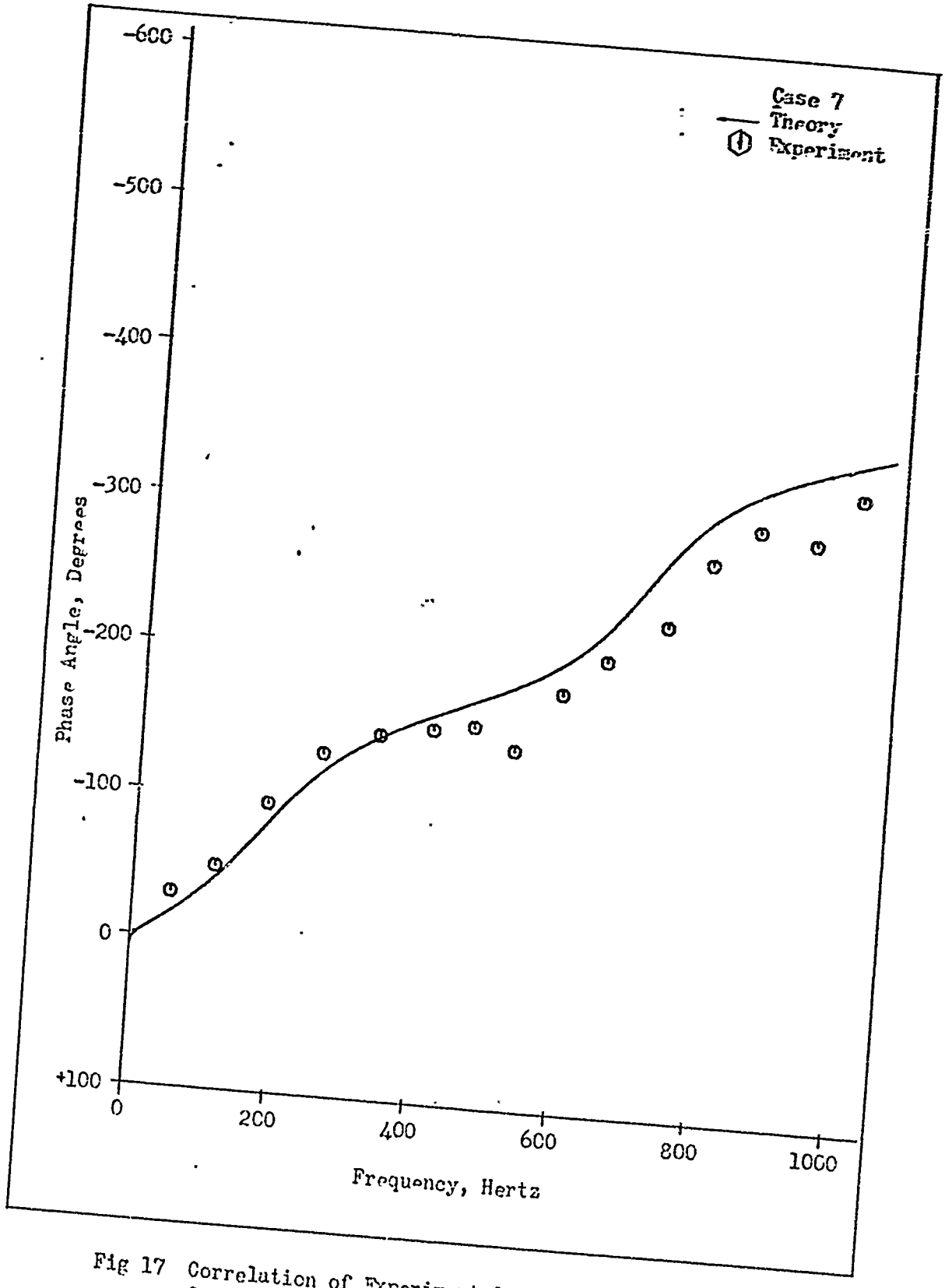

Fig 17 Correlation of Experimental Results with Theory for 0.0135 in ID orifice

mean turbulent flow cases by the use of these equations. The computer program used the equation that was nearest to the actual Reynolds number for its calculations, which allowed a maximum error of 250 Reynolds number for calculating the attenuation ratio, which would produce a maximum error in attenuation of approximately 10 percent. The curve labeled A in Figure 16 is the theoretical curve which was calculated using this increased attenuation. The results are much better than without increased attenuation, but agreement between theory and experiment is still lacking, especially at low frequencies. At frequencies above approximately 300 Hz, the results agree within ±2 db.

It was found by selectively reducing the orifice impedance, that agreement could be obtained between theory and experiment. It was also found, that this value of orifice impedance which caused theory and experiment to agree, could be obtained by modeling the orifice impedance differently than had been defined in equation (21), which was

$$Z_o = \frac{\overline{P}end}{Qend} + j0$$

which used the pressure at the end of the line divided by the flow rate at the end of the line. It was found that if the orifice impedance was modeled as

$$Z_o = \frac{\overline{P}end}{Qfm} + j0 \qquad (29)$$

which uses the flow rate at the flow meter expanding to atmospheric pressure, then good results could be obtained for the mean turbulent flow cases. The flow rate Qfm is larger than Qend, which gives a smaller Z_o. Values of $\overline{P}end$, Qend, and Qfm can be found in Table II for all test cases. The curve labeled Z in Figure 16 is the theoretical curve which

was calculated using increased attenuation, plus equation (29) was used to model the orifice impedance instead of equation (21). As can be seen in Figure 16, the results using both increased attenuation and reduced orifice impedance gives good results (within ±2 db) for the 0.0135 in ID orifice. Other results for the 0.0135 in ID orifice and the 0.016 and 0.020 in ID orifices can be found in Appendix A. It appears that as the orifice size becomes greater than one-half the ID of the main line with a mean turbulent flow, that the experimental results tend to differ more from theory, than for orifice sizes smaller than or equal to one-half the ID of the main line. Dynamic pressure phase shift for the turbulent mean flow cases tended to differ more from theory at high frequency, but agreed well at low frequency. These results for all of the turbulent mean flow cases can be seen in Figure 17 and Appendix A. Experimental results were still within ±70 degrees of the theoretical phase shift for mean turbulent flow. It appears some correction is needed for the phase shift as the mean flow rate increases.

VI. Conclusions

1. The computer program based on Nichols' equations and Kriebmaier and Lechner's modification to these equations predicts a dynamic pressure gain, which compares well with experiment for blocked lines, or for lines with a mean laminar flow at low signal sizes. Experimental gains agreed within ±1 db with theory over the frequency range, 40-1050 Hz.

2. Experimental dynamic pressure phase angle shift for this frequency range for blocked and mean laminar flow lines agreed with theory within ±15° for blocked flow and within ±30° when there was a mean laminar flow in the line.

3. The experimental dynamic pressure gain results for the transition region of mean flow agreed with the above theory within ±4 db.

4. Using increased attenuation when mean turbulent flow is present gives experimental dynamic pressure gain results which are within ±2 db of theory for orifice ID less than one-half the main line ID, if the orifice impedance is modeled as

$$Z_o = \frac{\overline{P}_{end}}{Q_{fm}} + j0$$

5. As signal size increases above 0.5 percent, the difference between experimental and theoretical results increases.

6. Dynamic pressure phase angle measurements could not be obtained on the oscilloscope in mean transition flow.

7. Experimental dynamic pressure phase angle measurements taken during mean turbulent flow tend to be less than predicted by theory by ±70° at high frequencies.

VII. Recommendations

1. Investigations should be undertaken of more complex networks to determine if the theory as developed for mean turbulent flow can be used in these networks to find dynamic pressure gain and phase shift.

2. Increased turbulent mean flow studies should be undertaken, and at frequencies above 1050 Hz.

3. Further studies of the effect of turbulent mean flow on dynamic pressure phase angles should be made.

4. Some means should be found to model the orifice impedance for mean turbulent flow which uses values of pressure and flow rate at one point, instead of the pressure at the orifice entrance and the flow rate at the orifice exit.

Bibliography

1. Bergh, H. and H. Tijdeman. Theoretical and Experimental Results for the Dynamic Response of Pressure Measuring Systems. National Aero- and Astronautical Research Institute Report No. NLR-TR F.238. Amsterdam: National Aero-and Astronautical Research Institute, January 1965.

2. Brown, F.T. "The Transient Response of Fluid Lines." Journal of Basic Engineering, Trans. ASME, 84:547-553 (December 1962).

3. Brown, F. T. et al. "Small Amplitude Frequency Behavior of Fluid Lines with Turbulent Flow." Journal of Basic Engineering, Trans. ASME, 91:678-693 (December 1969).

4. Foster, K. and J. E. Carley. "Analysis of Branched Pneumatic Transmission Lines Employed in High Frequency External Feedback Oscillators." Paper presented at the Fourth Cranfield Fluidics Conference: Warwich University, Coventry, England (March 1970).

5. Franke, M. E. et al. "Experimental Frequency Response of Fluidic Transmission Lines." Paper presented at the Fourth Cranfield Fluidics Conference: Warwich University, Coventry, England (March 1970).

6. Franke, M. E. et al. "The Frequency Response of Volume-Terminated Pneumatic Lines with Circular and Rectangular Cross Sections." Paper presented at the 1969 Joint Automatic Control Conference, Boulder, Colorado, August 1969.

7. Hammond, W. R., Jr. Investigation of Dynamic Characteristics of Fluid Transmission Lines with Flow. Unpublished Thesis. Wright-Patterson Air Force Base, Ohio: Air Force Institute of Technology, 1970.

8. Iberall, A. S. "Attenuation of Oscillatory Pressures in Instrument Lines." Journal of Research, 45:85-108 (1950).

9. Karam, J. T., Jr. The Frequency Response of Blocked Pneumatic Lines. Unpublished Thesis. Wright-Patterson Air Force Base, Ohio: Air Force Institute of Technology, 1966.

10. Karam, J. T., Jr. and M. E. Franke. "The Frequency Response of Pneumatic Lines." Journal of Basic Engineering, Trans. ASME, 89: 371-378 (June 1967).

11. Krishnaiyer, R. and T. J. Lechner, Jr. "An Experimental Evaluation of Fluidic Transmission Line Theory." Advances in Fluidics. Edited by F. T. Brown et al. New York: American Society of Mechanical Engineers, 1967.

12. Malanowski, A. J. The Dynamic Response of Fluidic Networks. Unpublished Thesis. Wright-Patterson Air Force Base, Ohio: Air Force Institute of Technology, 1971.

13. Martin, P. S. Temperature Effects on the Dynamic Characteristics of Blocked Cascaded Pneumatic Transmission Lines. Unpublished Thesis. Wright-Patterson Air Force Base, Ohio: Air Force Institute of Technology, 1970.

14. Miller, R. N. Dynamic Characteristics of Blocked, Concentric, Cascaded Pneumatic Transmission Lines. Unpublished Thesis. Wright-Patterson Air Force Base, Ohio: Air Force Institute of Technology, 1968.

15. Morse, P. M. and K. U. Ingard. Theoretical Acoustics. New York: McGraw Hill Book Co., Inc., 1968.

16. Nichols, N. B. "The Linear Properties of Pneumatic Transmission Lines." Transactions of the Instrument Society of America, 1:5-14 (January 1962).

17. Ramo, S. et al. Fields and Waves in Communication Electronics. New York: John Wiley and Sons, Inc., 1965.

18. Rohmann, C. P. and E. C. Grogan. "On the Dynamics of Pneumatic Transmission Lines." Transactions of the American Society of Mechanical Engineers, 79:853-874 (May 1957).

19. Skilling, H. H. Electric Transmission Lines. New York: McGraw-Hill Book Co., Inc., 1951.

20. Wilda, R. H. Pneumatic Line Dynamics. Unpublished Thesis. Wright-Patterson Air Force Base, Ohio: Air Force Institute of Technology, 1967.

Appendix A

Frequency Response Curves Correlating Theory with Experimental Results

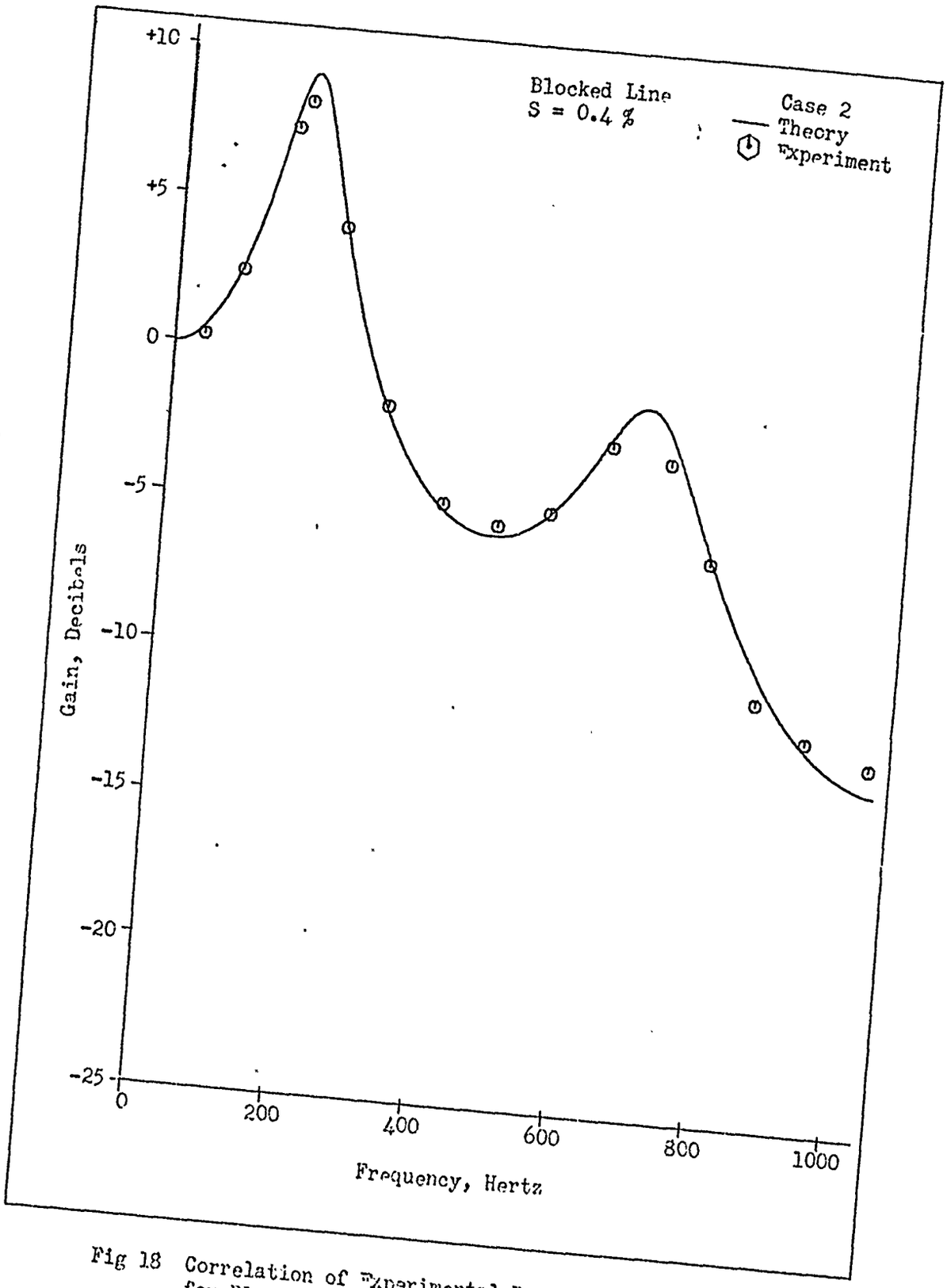

Fig 18 Correlation of Experimental Results with Theory for Blocked Line

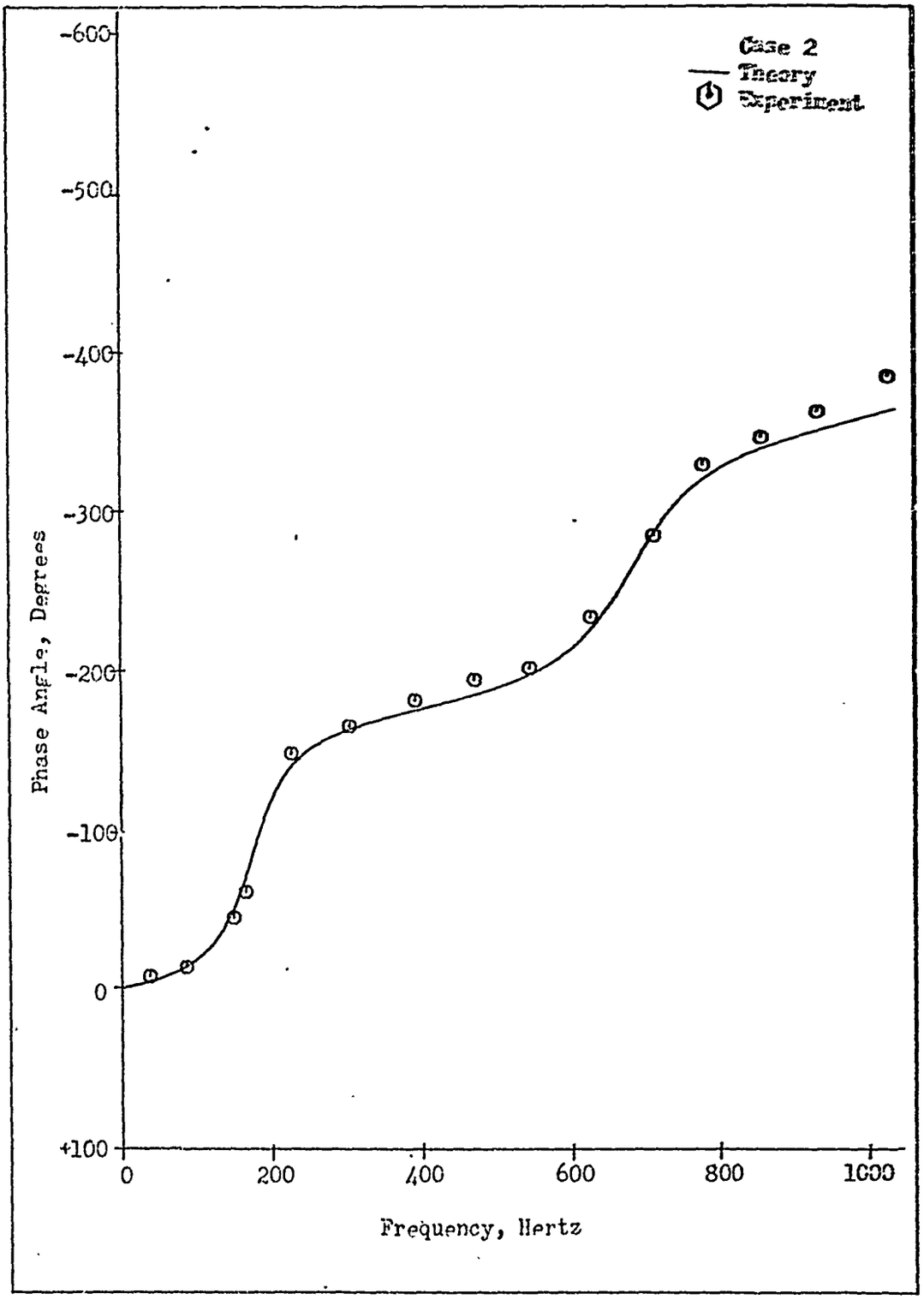

Fig 19 Correlation of Experimental Results with Theory for Blocked Line

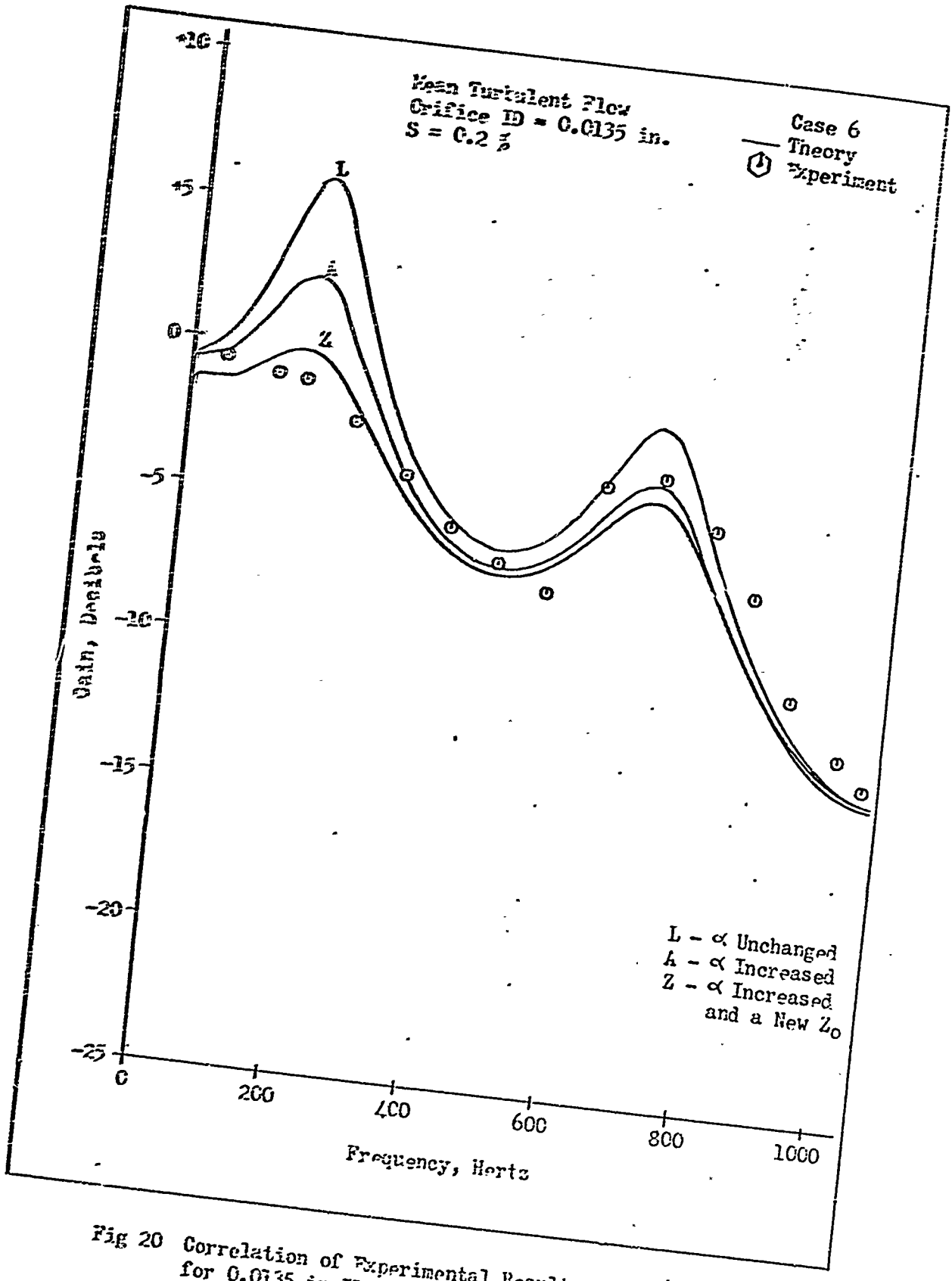

Fig 20 Correlation of Experimental Results with Theory for 0.0135 in ID orifice

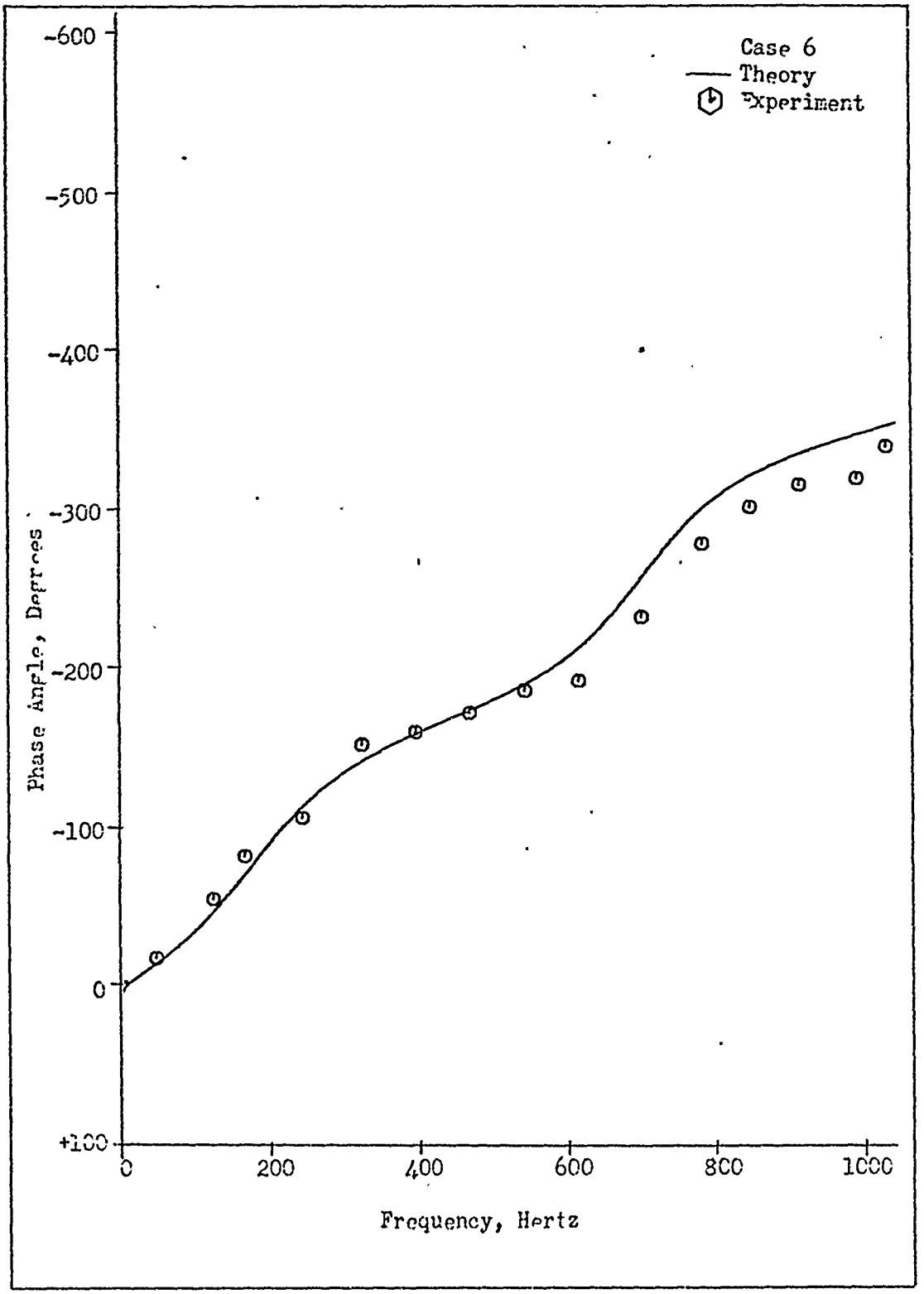

Fig 21 Correlation of Experimental Results with Theory for 0.0135 in ID orifice

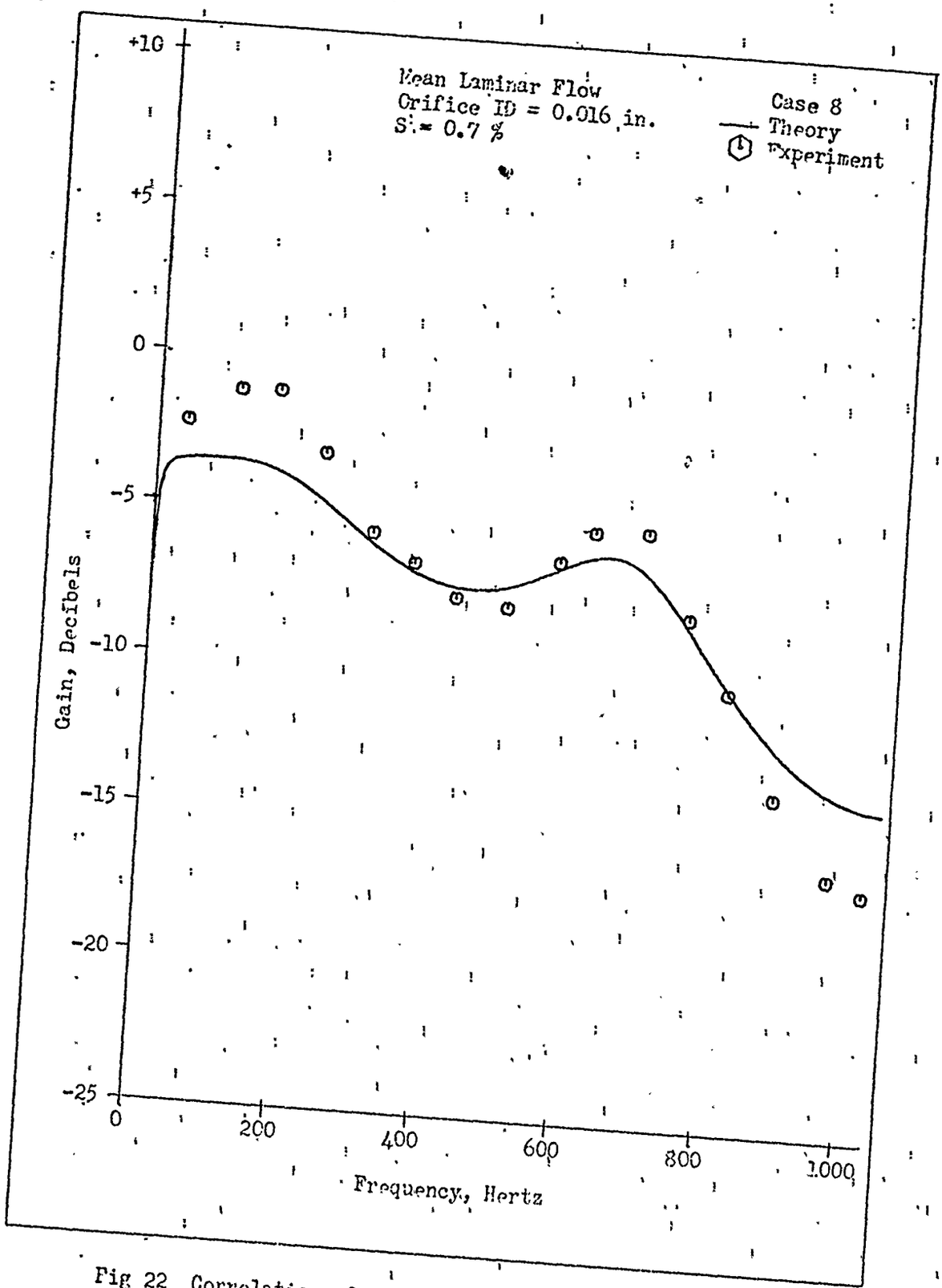

Fig 22 Correlation of Experimental Results with Theory for 0.016 in ID orifice

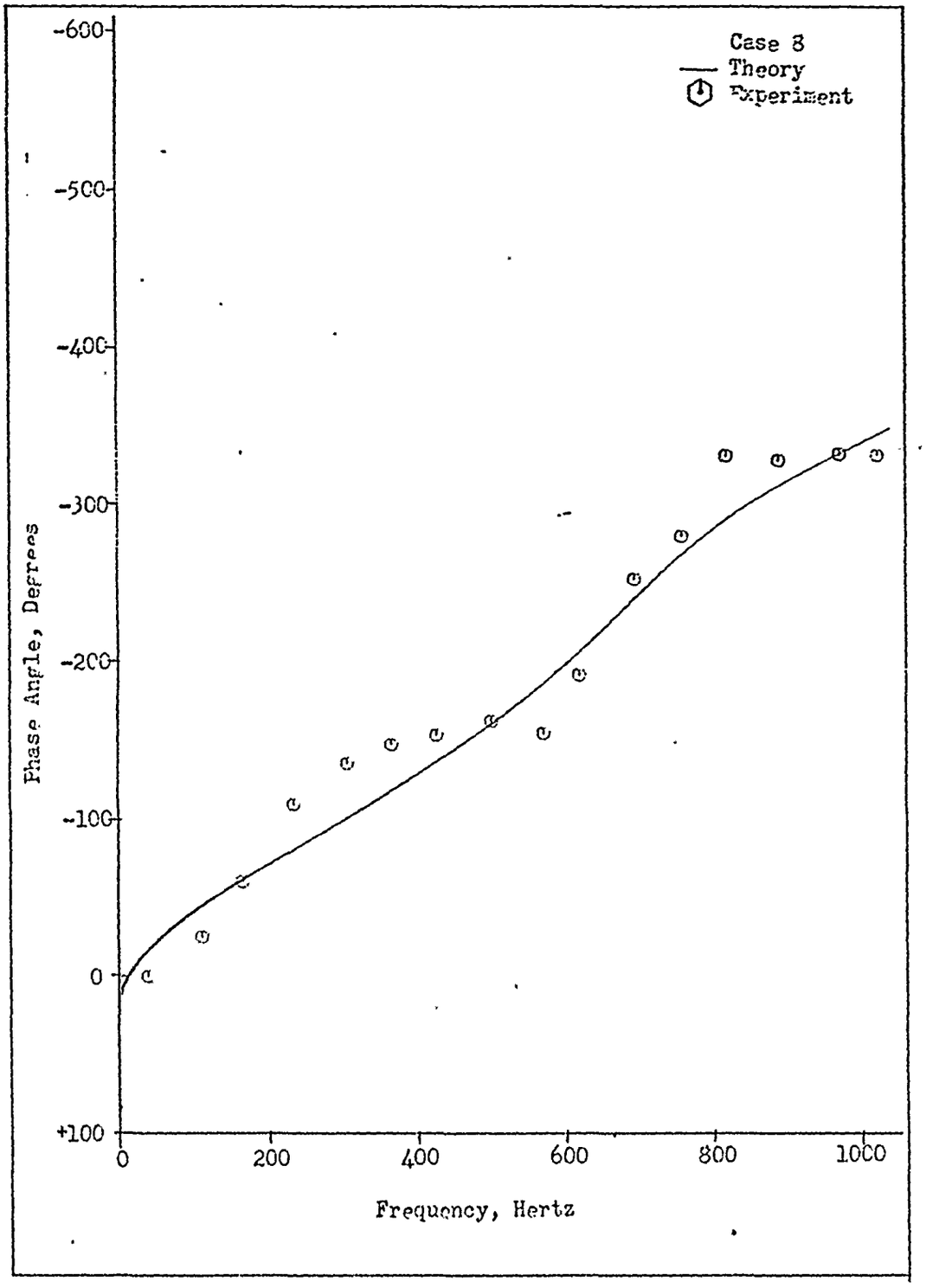

Fig 23 Correlation of Experimental Results with Theory for 0.016 in ID orifice

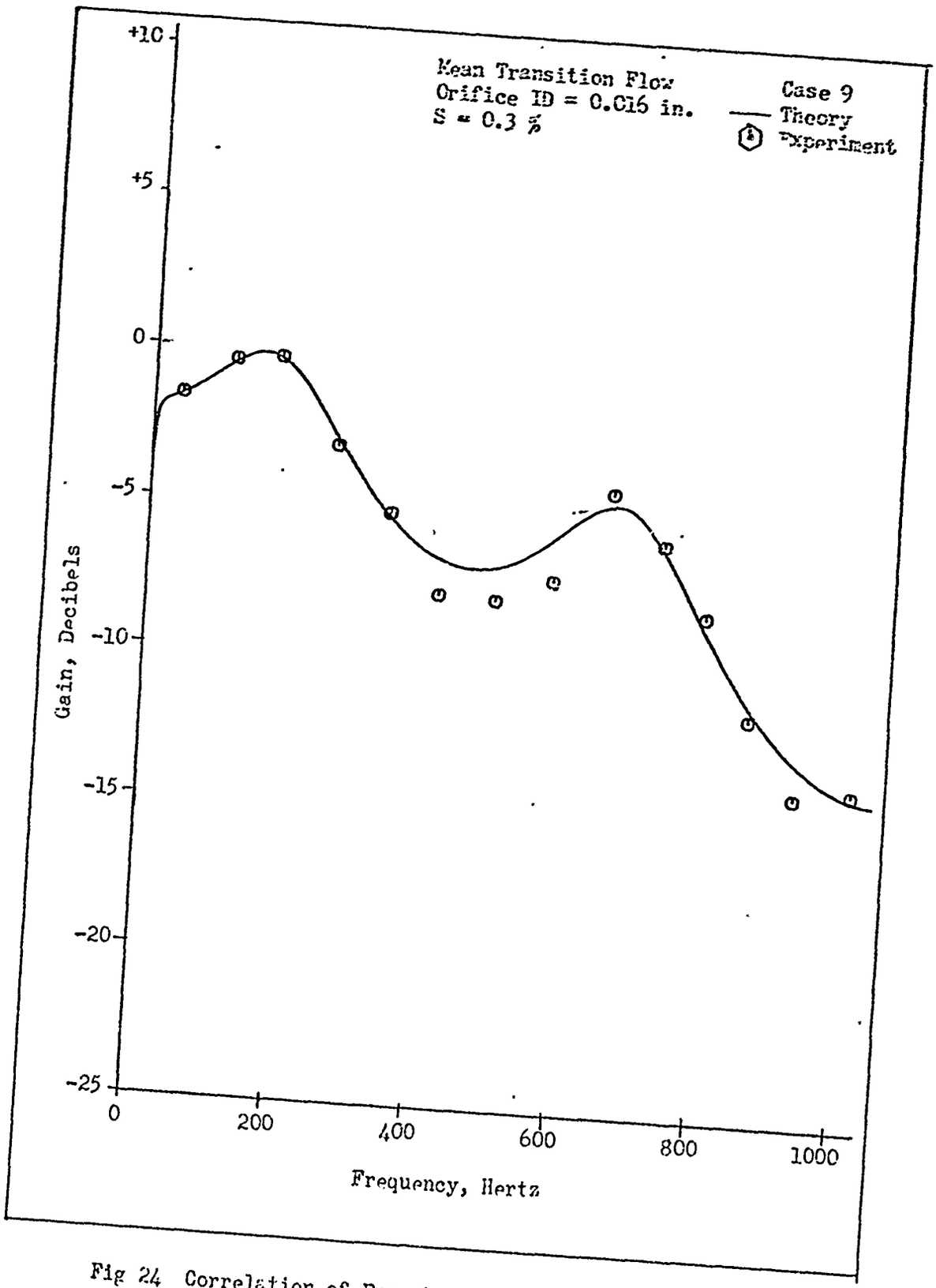

Fig 24 Correlation of Experimental Results with Theory for 0.016 in ID orifice

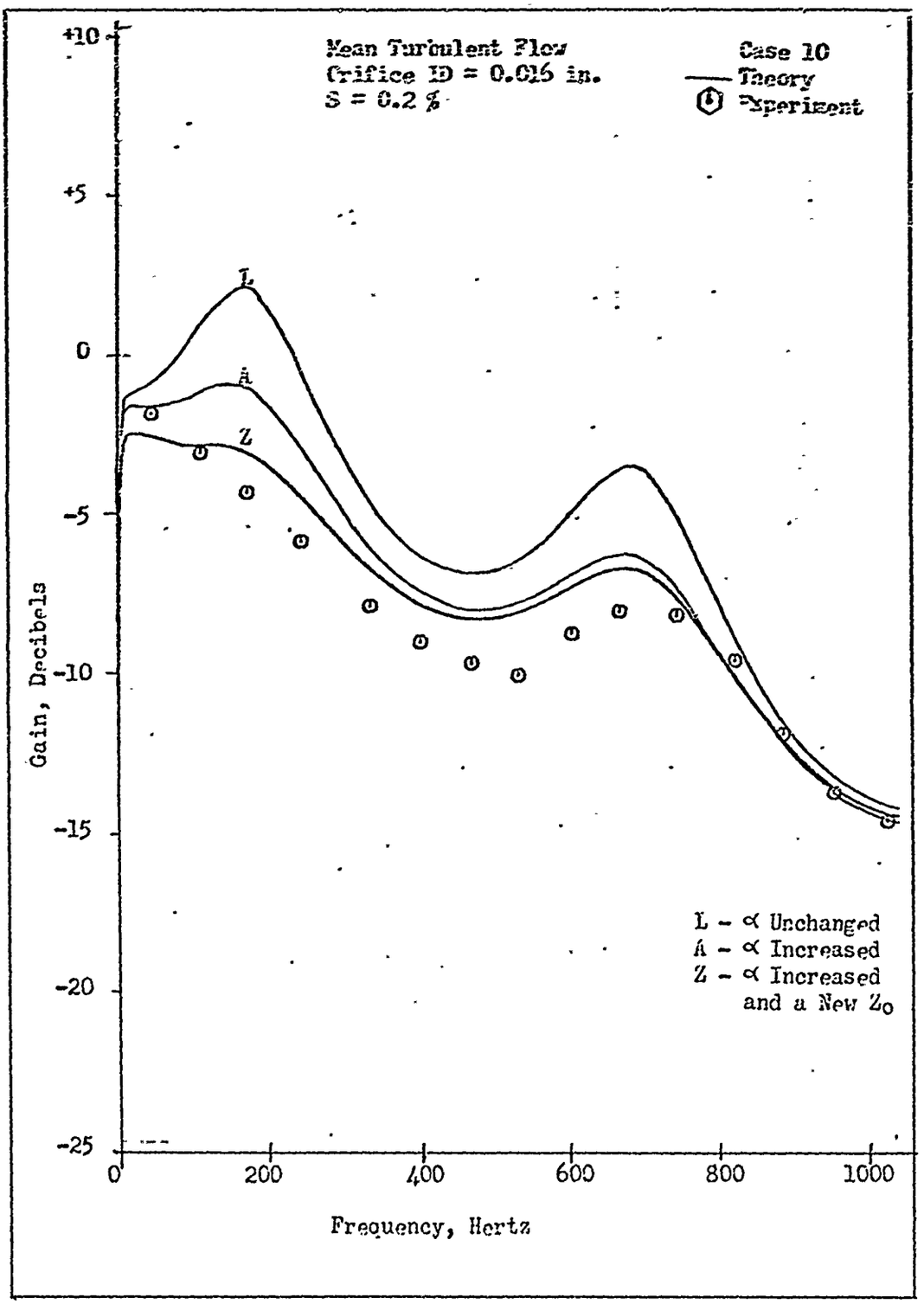

Fig 25 Correlation of Experimental Results with Theory for 0.016 in ID orifice

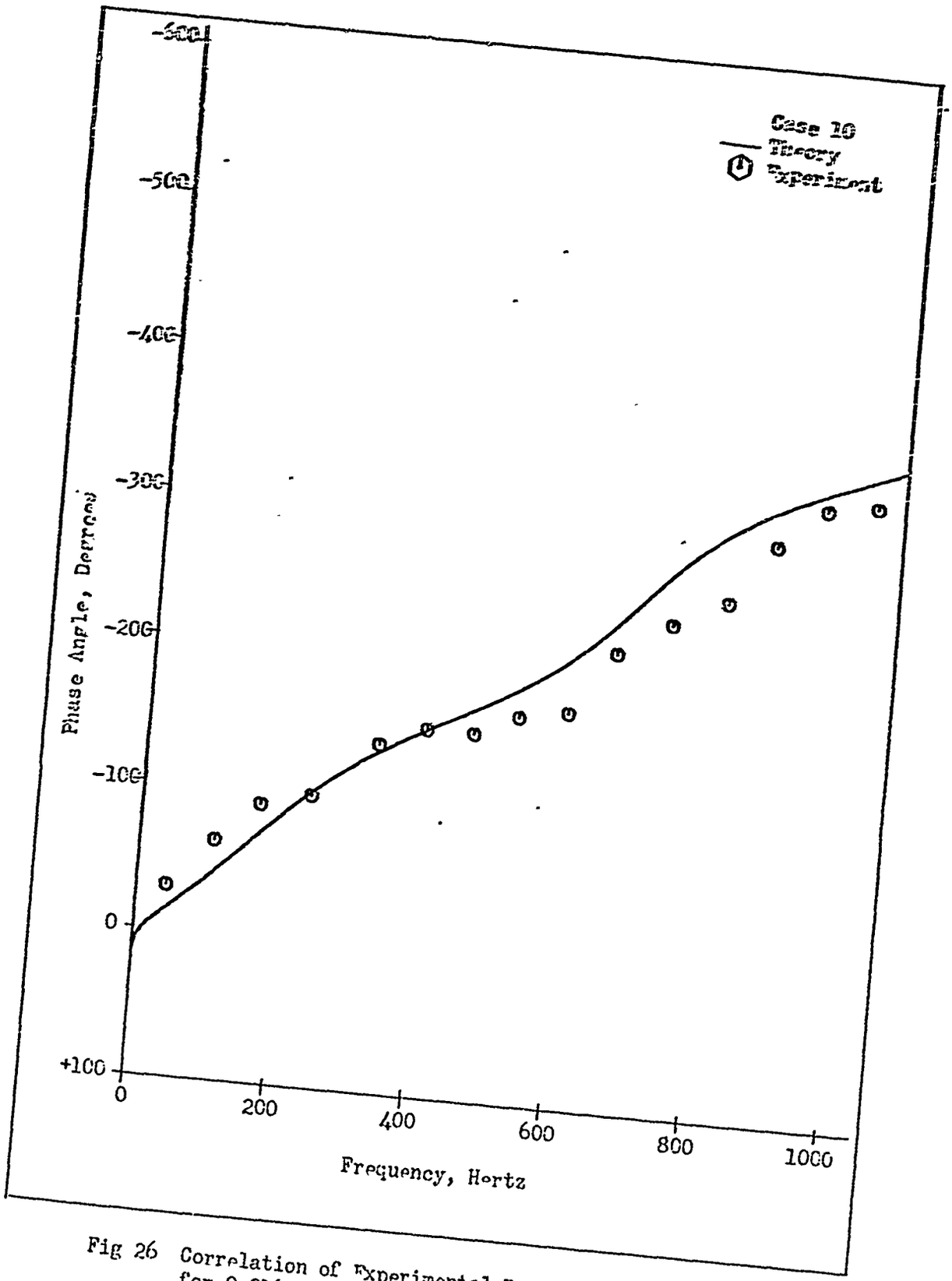

Fig 26 Correlation of Experimental Results with Theory for 0.016 in ID orifice

GA/MF/72-2

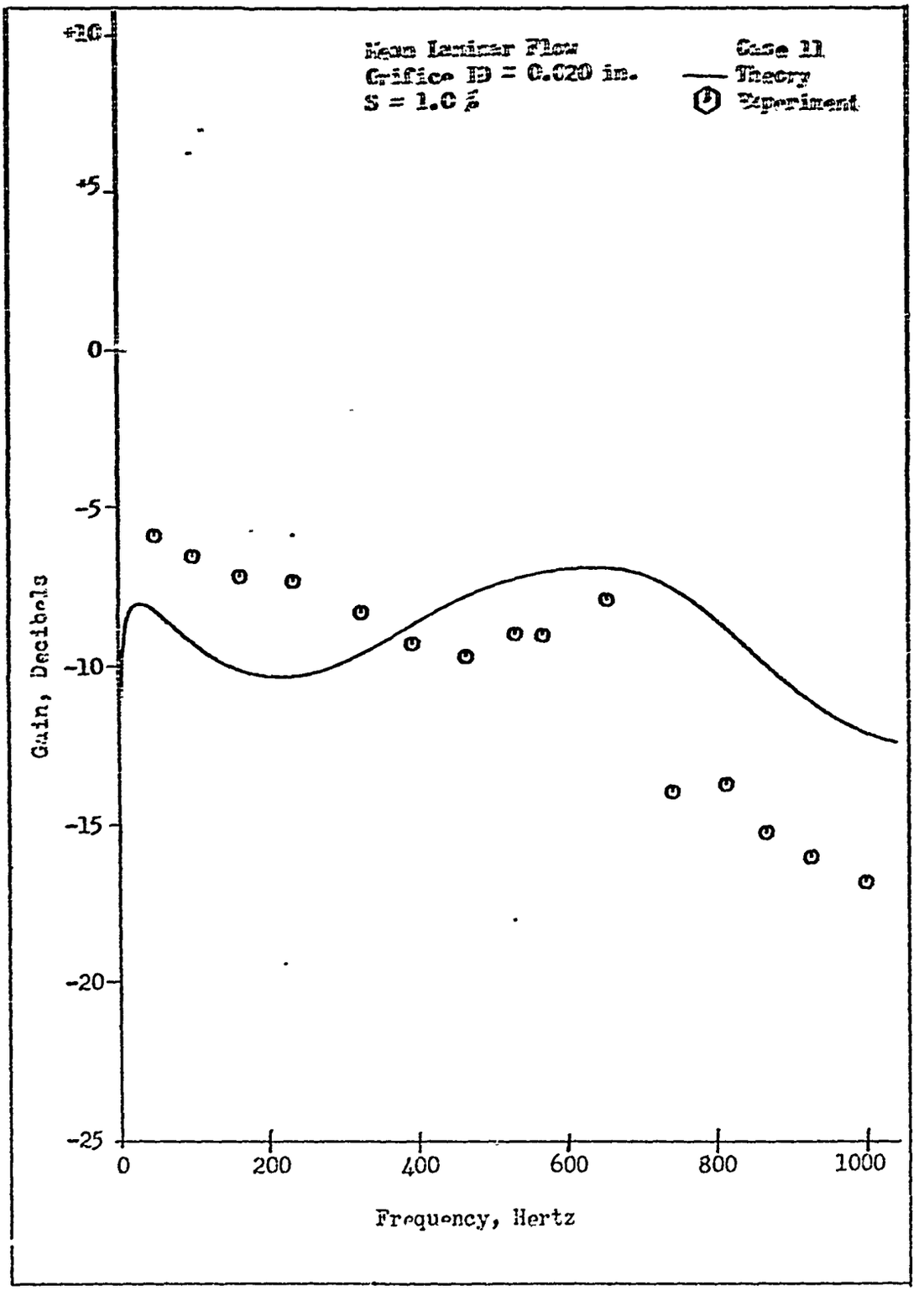

Fig 27 Correlation of Experimental Results with Theory for 0.020 in ID orifice

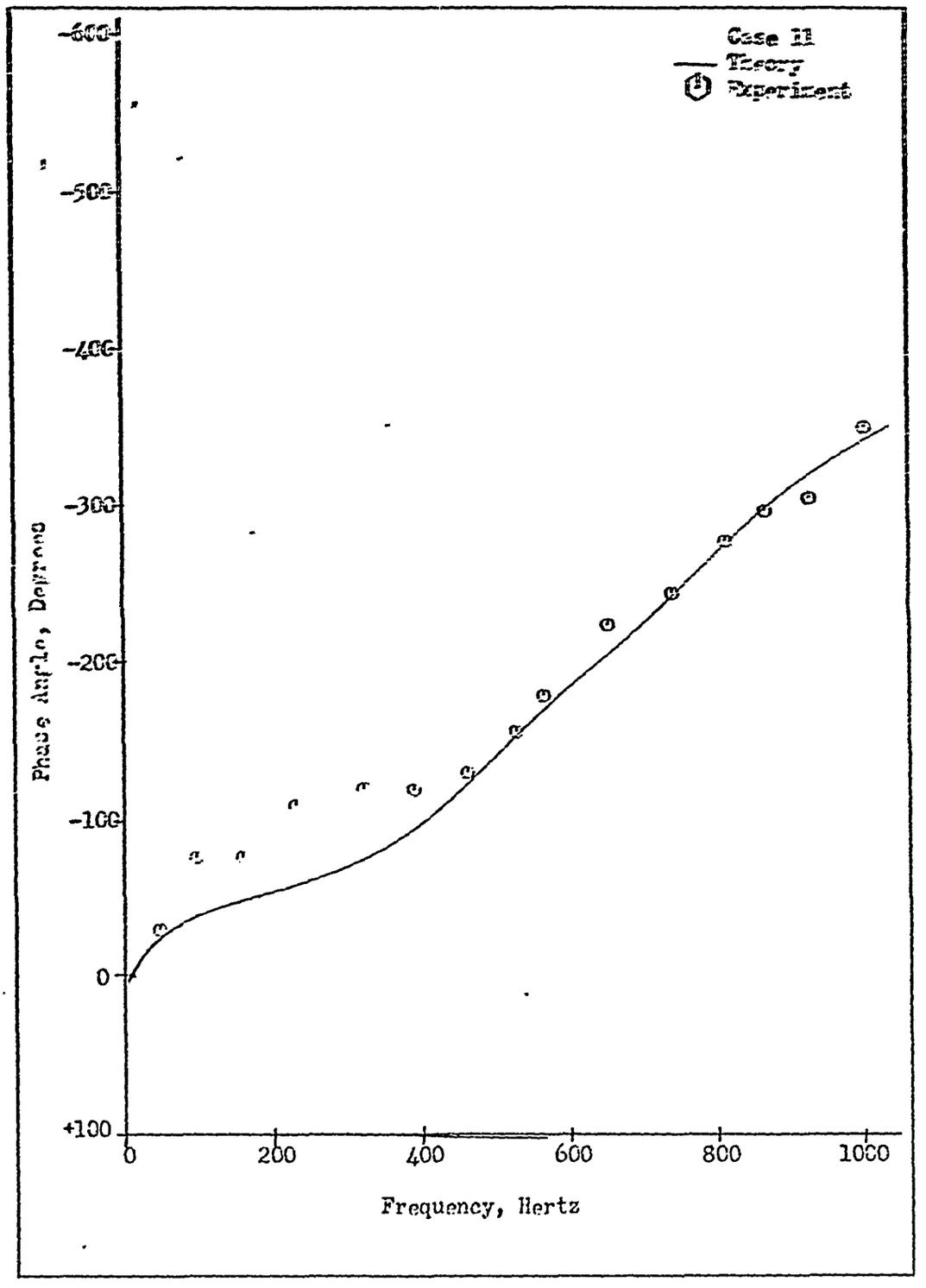

Fig 28 Correlation of Experimental Results with Theory for 0.020 in ID orifice

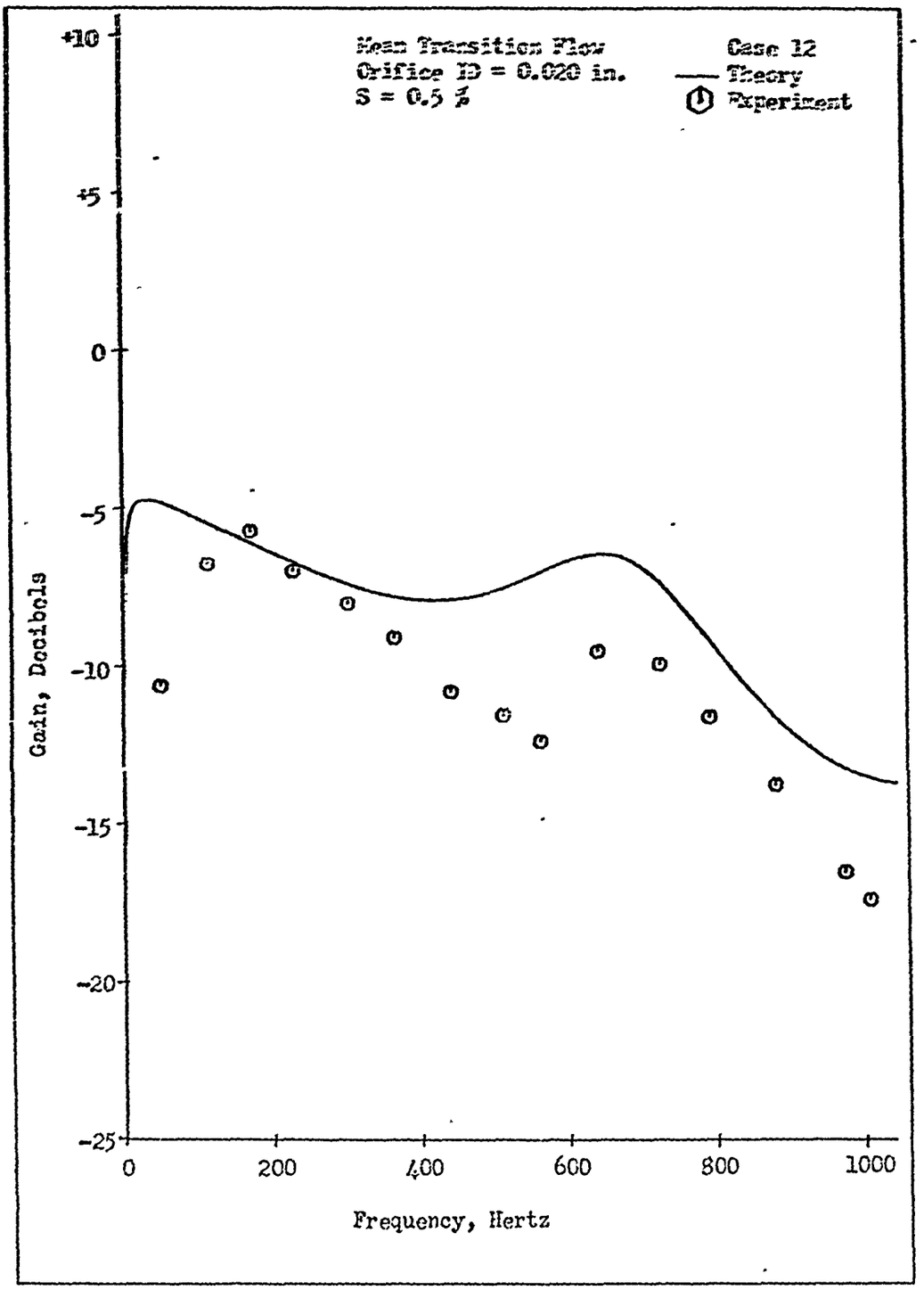

Fig 29 Correlation of Experimental Results with Theory for 0.020 in ID orifice .

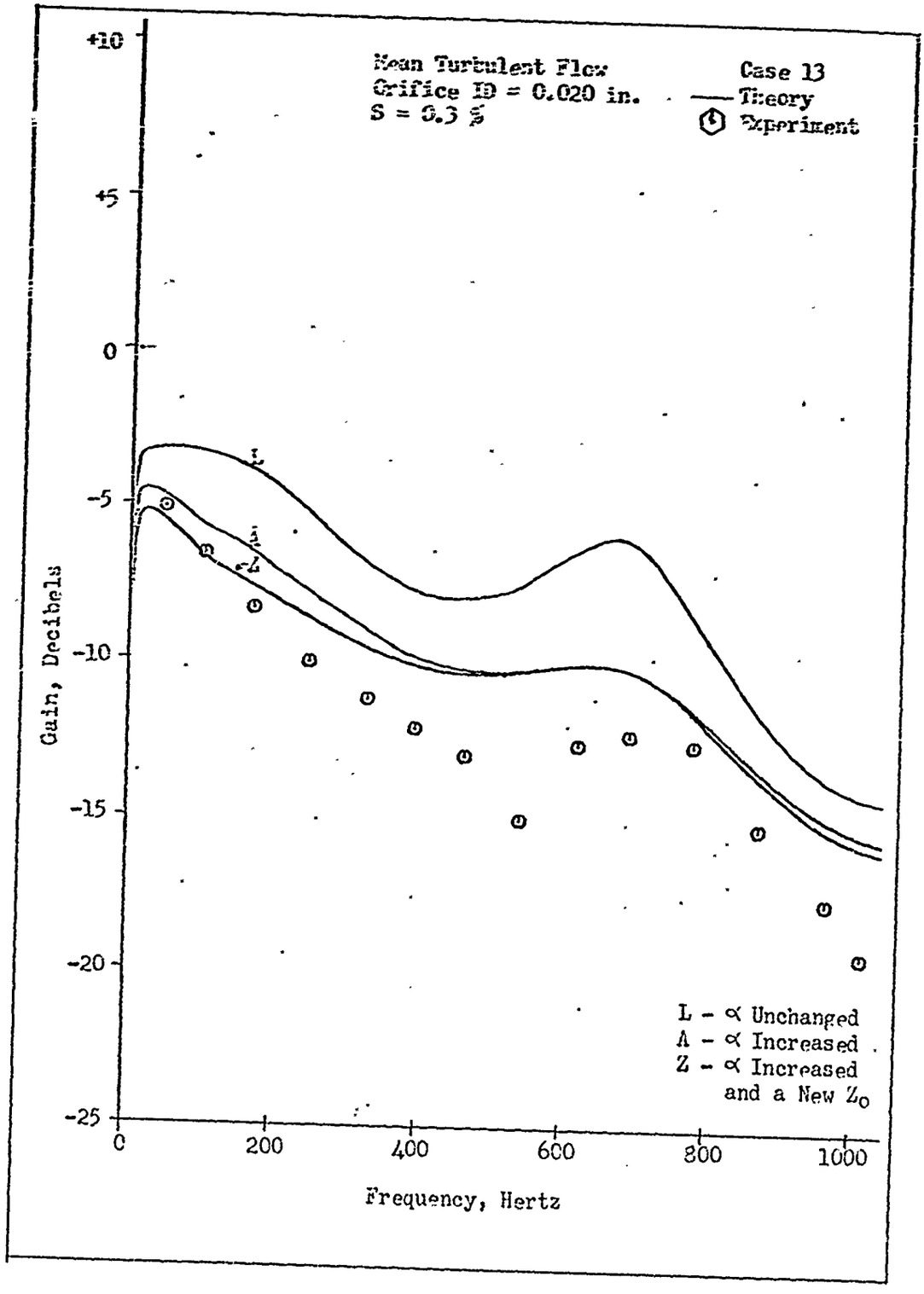

Fig 30 Correlation of Experimental Results with Theory for 0.020 in ID orifice

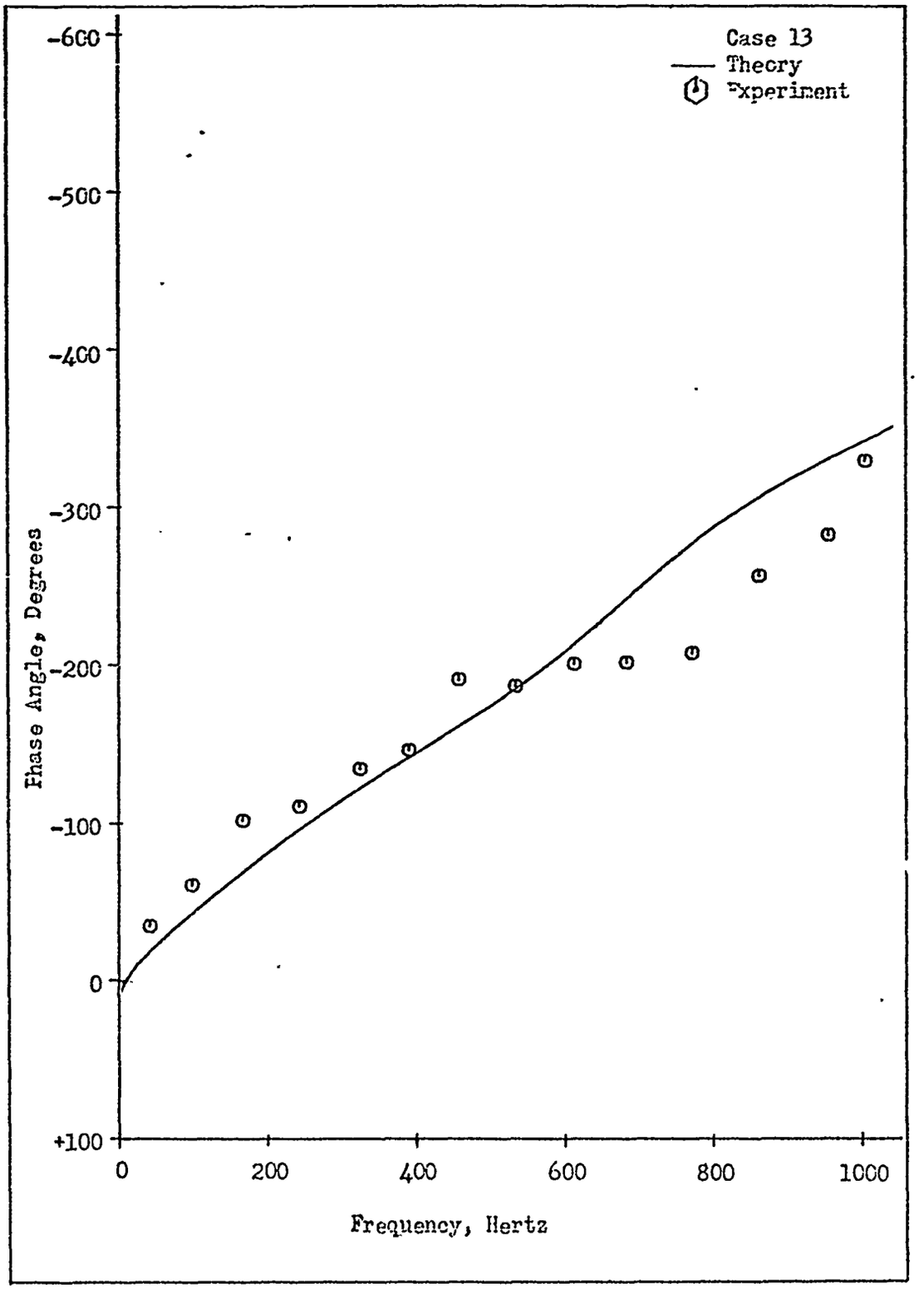

Fig 31 Correlation of Experimental Results with Theory for 0.020 in ID orifice

Appendix B

Complete Line Dimensions

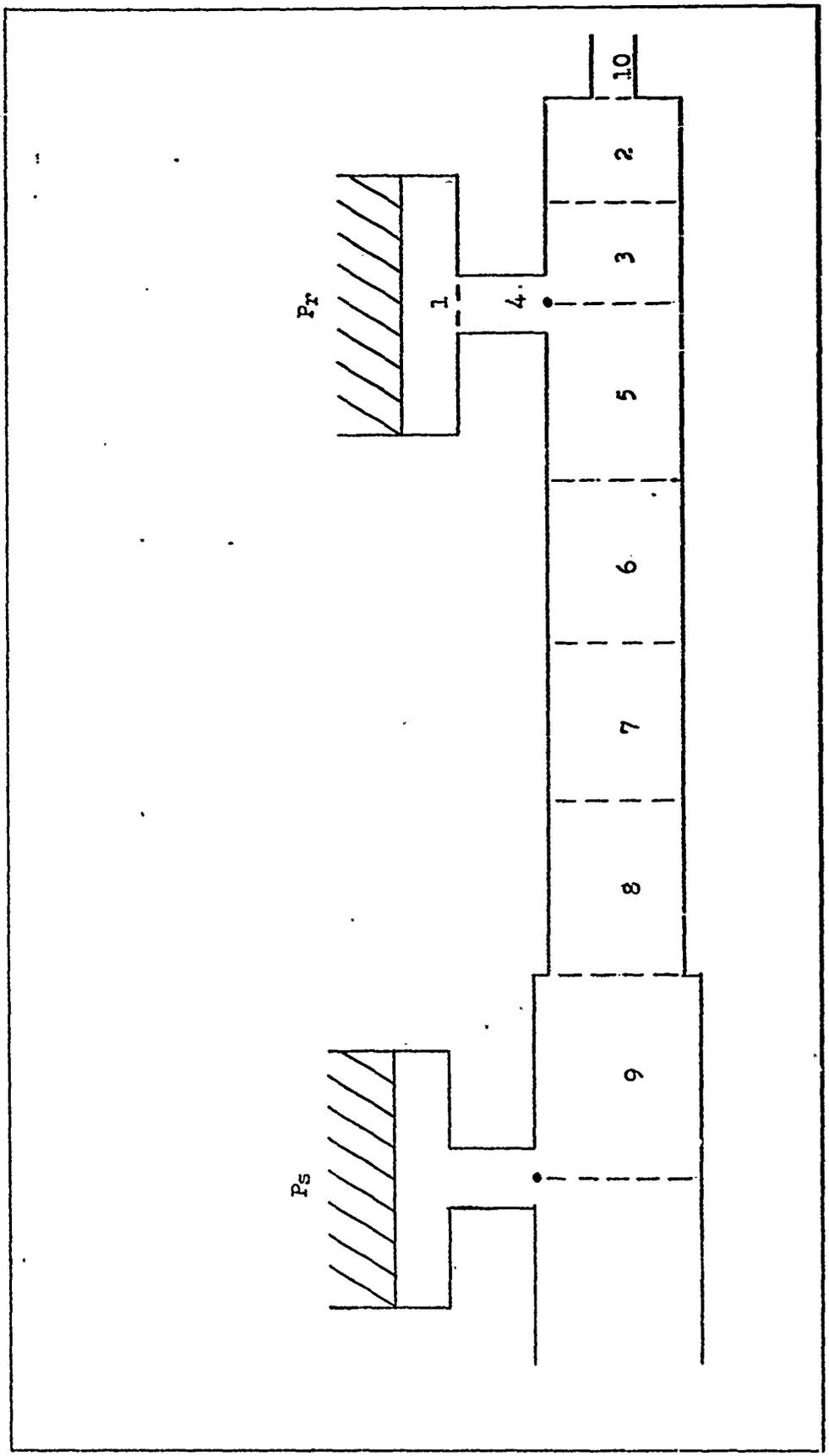

Fig 32 Schematic Diagram of Line Configuration

Table III

Case 1 and 2

Line Section	Diameter in.	Length in.
1	0.3750	0.040
2	0.0320	0.490
3	0.0320	0.500
4	0.0320	0.156
5	0.0320	2.500
6	0.0320	2.500
7	0.0320	2.500
8	0.0320	2.470
9	0.0625	0.030
10	0.0000	0.000

Table IV

Case 3,4,5,6 and 7

Line Section	Diameter in.	Length in.
10	0.0135	0.062
Remainder are the same as Case 1		

Table V

Case 8,9 and 10

Line Section	Diameter in.	Length in.
10	0.0160	0.062
Remainder are the same as Case 1		

Table VI

Case 11,12 and 13

Line Section	Diameter in.	Length in.
10	0.0200	0.062
Remainder are the same as Case 1		

Vita

Bradley O. Montgomery was born on 17 May 1941 in Buckhannon, West Virginia, the son of Earl Joseph and Marjorie Ruth Montgomery. He graduated from Buckhannon-Upshur High School, Buckhannon, West Virginia in 1959, and entered the Air Force in August of 1959. While stationed at Dow Air Force Base, Maine, he attended the University of Maine. After six years in Maine, he was stationed at Blytheville Air Force Base, Arkansas where he completed enough courses on base through Southern Baptist College to apply for the Airman's Educationing and Commissioning Program. He was accepted and sent to Oklahoma State University in August 1967, where he received his Bachelor of Science in Aerospace Engineering in January, 1970. After completion of Officer's Training School at Lackland Air Force Base, Texas, in April 1970, he was assigned to the Air Force Institute of Technology, Wright-Patterson Air Force Base, Ohio.

Permanent Address: Route 2, Box 140
Buckhannon, West Virginia 26201